Published in final edited form as:
Dev Biol. 2013 November 1; 383(1): 106–120. doi:10.1016/j.ydbio.2013.08.014.

Smurf-mediated differential proteolysis generates dynamic BMP signaling in germline stem cells during *Drosophila* testis development

Yi-Jie Chang[a,b,1], **Haiwei Pi**[a,b,*,1], **Chang-Che Hsieh**[a,b], and **Margaret T. Fuller**[c]

[a]Graduate Institute of Biomedical Sciences, College of Medicine, Chang Gung University, 259 Wen-Hwa 1st Road, Kwei-Shan, Tao-Yuan 333, Taiwan

[b]Department of Biomedical Sciences, College of Medicine, Chang Gung University, 259 Wen-Hwa 1st Road, Kwei-Shan, Tao-Yuan 333, Taiwan

[c]Department of Developmental Biology, Stanford University, School of Medicine, Stanford, CA 94305, USA

Abstract

Germline stem cells (GSCs) produce gametes throughout the reproductive life of many animals, and intensive studies have revealed critical roles of BMP signaling to maintain GSC self-renewal in *Drospophila* adult gonads. Here, we show that BMP signaling is downregulated as testes develop and this regulation controls testis growth, stem cell number, and the number of spermatogonia divisions. Phosphorylated Mad (pMad), the activated *Drosophila* Smad in germ cells, was restricted from anterior germ cells to GSCs and hub-proximal cells during early larval development. pMad levels in GSCs were then dramatically downregulated from early third larval instar (L3) to late L3, and maintained at low levels in pupal and adult GSCs. The spatial restriction and temporal down-regulation of pMad, reflecting the germ cell response to BMP signaling activity, required action in germ cells of E3 ligase activity of HECT domain protein Smurf. Analyses of *Smurf* mutant testes and dosage-dependent genetic interaction between *Smurf* and *mad* indicated that pMad down-regulation was required for both the normal decrease in stem cell number during testis maturation in the pupal stage, and for normal limit of four rounds of spermatogonia cell division for control of germ cell numbers and testis size. Smurf protein was expressed at a constant low level in GSCs and spermatogonia during development. Rescue experiments showed that expression of exogenous Smurf protein in early germ cells promoted pMad downregulation in GSCs in a stage-dependent but concentration-independent manner, suggesting that the competence of Smurf to attenuate response to BMP signaling may be regulated during development. Taken together, our work reveals a critical role for differential attenuation of the response to BMP signaling in GSCs and early germ cells for control of germ cell number and gonad growth during development.

*Corresponding author at: Department of Biomedical Sciences, College of Medicine, Chang Gung University, 259 Wen-Hwa 1st Road, Kwei-Shan, Tao-Yuan 333, Taiwan. haiwei@mail.cgu.edu.tw (H. Pi).
[1]These two authors contribute equally to this work.

Appendix A. Supporting information

Supplementary data associated with this article can be found in the online version at http://dx.doi.org/10.1016/j.ydbio.2013.08.014.

Keywords

Drosophila; Spermatogenesis; Germline stem cells; BMP; Smurf; Proteolysis

Introduction

Adult stem cells play key roles in maintaining populations of short-lived but highly differentiated cell types throughout life. Proper regulation of the number of active stem cells and/or the number of rounds of transient amplifying mitotic divisions of their differentiating progenies by developmental or physiological changes or in response to wounding is important for tissue homeostasis and tissue size.

Spermatogenesis in *Drosophila* has emerged as the premier system for studying regulation of adult stem cells and their differentiating progenies (reviewed in Davies and Fuller, 2008; Yamashita et al., 2010). In the testis, all the germ cells are derived from a small number of germline stem cells (GSCs). Each testis contains 7–9 GSCs that form a ring surrounding a cluster of somatic cells known as the hub. The germ cells adherent to the hub normally maintain GSC identity and orient the mitotic spindles perpendicular to the GSC–hub interface. The asymmetric GSC division normally gives rise to one daughter cell that maintains the contact with the hub and GSC identity, and one daughter cell that is normally displaced away from the hub and initiates differentiation as a goniablast (Gb). Each Gb initiates exactly four rounds of transit-amplifying (TA) divisions to produce a cyst with 16 interconnecting germ cells, which exit the mitotic program in synchrony and commit to spermatocyte differentiation.

GSC maintenance requires activation of the BMP signaling pathway within germ cells. The BMP ligands Gbb and Dpp expressed in hub cells at the tip of the testis activate the receptor Tkv at the GSC–hub interface (Kawase et al., 2004; Michel et al., 2011; Shivdasani and Ingham, 2003). Gbb and Dpp are also expressed in the cyst cells including the cyst stem cells, which flank the GSCs and are essential for GSC renewal (Kawase et al., 2004; Leatherman and DiNardo, 2008; Leatherman and Dinardo, 2010; Shivdasani and Ingham, 2003). In testes carrying germ line clones mutant for components necessary for response to BMP signaling, such as *tkv* (type I receptor), *punt* (type II receptor), *mad* (SMAD) or *medea* (co-SMAD), GSCs are completely lost within two weeks (Kawase et al., 2004; Shivdasani and Ingham, 2003). BMP signaling activity in early germ cells also controls timing of the switch from TA mitotic proliferation to spermatocyte differentiation, as TA cells could enter spermatocyte differentiation before the fourth round of mitosis in *tkv* mutant cysts (Shivdasani and Ingham, 2003), and forced expression of Dpp or the constitutively active Tkv in all spermatogonia causes continuous division of TA cells at the expense of the switch to spermatogonia differentiation program (Bunt and Hime, 2004; Kawase et al., 2004; Schulz et al., 2004). BMP signaling is thought to promote TA division by blocking the expression of *bag of marbles* (*bam*) (Chen and McKearin, 2003a, 2003b; Gonczy et al., 1997; Kawase et al., 2004; Shivdasani and Ingham, 2003), a key regulator for termination of TA division and initiation of spermatocyte differentiation (McKearin and Spradling, 1990).

Although much is known how the BMP pathway is activated during male germline development (Kawase et al., 2004; Michel et al., 2011), how BMP signaling is negatively regulated and the consequences of such negative regulation is unknown. One of the key negative regulators for the BMP pathway is the HECT domain ubiquitin E3 ligase SMAD ubiquitination regulatory factor (Smurf). Smurf was first identified as a SMAD1-interacting protein involved in SMAD poly-ubiquitination and degradation, thus regulating the output of the BMP pathway (Kavsak et al., 2000; Lin et al., 2000; Zhang et al., 2001; Zhu et al., 1999). Smurf is sufficient to suppress response to BMP pathway in *Xenopus* embryos (Zhu et al., 1999). Likewise, in *Drosophila*, loss of *Smurf* activity results in expansion and prolongation of Dpp signaling in embryonic D–V patterning and gut organogenesis (Podos et al., 2001). In *Drosophila* adult female germline, Smurf action appears to limit the number of germ cells responsive to Dpp and promote differentiation of the cystoblast, the female GSC daughter cell that initiates differentiation (Casanueva and Ferguson, 2004; Xia et al., 2010). There are two Smurf homologs, Smurf1 and Smurf2, in vertebrates (human, mice and *Xenopus*). In addition to the BMP pathway, Smurf1 and Smurf2 control diverse cellular behaviors such as polarity, mobility, planar cell polarity, axon formation and autophagy in higher animals by mediating degradation of substrates including RhoA, Par6, Prickle and MEKK2 (Cheng et al., 2011; Narimatsu et al., 2009; Orvedahl et al., 2011; Schwamborn et al., 2007a, 2007b; Wang et al., 2003; Yamashita et al., 2005).

In this study, we show that Smurf plays an important role in cell number control of GSCs and proliferating germ cells during male gonad development form larva to adult. During male gonad development, the earliest GSCs are specified from the primordial germ cells (PGCs) by the end of embryogenesis. In stage 17 embryos, the PGC to GSC transition occurs in the anterior germ cells that reside adjacent to the newly-formed apical hub (Sheng et al., 2009). The hub promotes GSC establishment through differential cell adhesion and induction of Jak-STAT pathway (Sheng et al., 2009). In this study, we found that BMP signaling, the key pathway for adult GSC maintenance, is spatially and temporally downregulated in stem cells and early germ cells in larval and pupal testes. This downregulation is mediated by the proteolytic activity of Smurf, in a developmental stage-dependent but concentration-independent mechanism. Down-regulation of BMP signaling by Smurf is essential for the normal decrease in stem cell number during pupal development, as well as for timely termination of spermatogonia proliferation program for control of germ cell number and testis size. Together, our results reveal an important role of differential proteolysis in regulation of dynamic BMP signaling activation and organ growth during male gonad development.

Material and methods

Fly strains

w^{1118} flies were used as wild-type. $Smurf^{15C}$ (Podos et al., 2001), mad^{12} (Sekelsky et al., 1995), mad^{1-2} (Wiersdorff et al., 1996), bam^{86} (McKearin and Ohlstein, 1995), fu^{mH63}, fu^{50} (fu^{G3}), fu^{52} (fu^{JB3}), fu^{54} (fu^{M1}) (Preat et al., 1993), stg^{4} (Edgar and O'Farrell, 1989), *stg-GFP*^{YD0685} (Inaba et al., 2011), *Dad-LacZ* (Dad^{P1883}) (Tsuneizumi et al., 1997), *nos-gal4-VP16* (Van Doren et al., 1998), *bam-gal4* (Chen and McKearin, 2003b), *hs-bam* (Ohlstein

and McKearin, 1997) and *UAS-EcRB1*$^{\Delta 655F645A}$ (Hu et al., 2003) were described previously. *Df*(*2R*)*Exel7149* is the smallest deletion line available from Bloomington stock center that uncovers *Smurf*. Clones and germline-specific clones of *Smurf*^{15C} were generated, respectively, in *hs-FLP*/*Y*; *FRT*^{42d} *Smurf*^{15C}/*FRT*^{42d} *arm-LacZ* and *UAS-FLP*/*Y*; *FRT*^{42d} *Smurf*^{15C}/*FRT*^{42d} *ubi-GFP*; *nos-Gal4*/+ flies. *UAS-myc-Smurf*, *UAS-flag-Smurf*^{C1029A} and *1.4-GFP* transgenic lines were generated by standard *P*-element mediated transformation.

Immunostaining

Testes were dissected in 1 × PBS and fixed in 4% paraformaldehyde for 20 min. After washing with 1 × PBT (Trion X-100, 0.3%), testes were permeabilized in 0.3% NaDoc (0.3% sodium deoxycholate, 0.3% Triton X-100, 1 × PBS) for 30 min. For immunostaining, testes were incubated with primary antibodies overnight at 4 °C in PBS buffer containing 0.3% BSA and 0.3% Trion X-100, followed by three washes and incubation with secondary antibodies for 1.5 h at RT. The following antibodies were used: rabbit anti-DSmurf at 1:200 (generated in this study), goat anti- Vasa at 1:250 (dc-13, Santa Cruz), rabbit anti-Vasa at 1:250 (d-260, Santa Cruz), mouse anti-FasIII at 1:50 (DSHB), mouse anti-Arm at 1:100 (DSHB), mouse anti-BamC at 1:5 (DSHB), rabbit anti-pSmad at 1:2000 to 1:5000 (a gift from Dr. Laufer) (Crickmore and Mann, 2006), mouse anti-β-galactosidase at 1:250 (40-1a, DSHB), rabbit anti-GFP at 1:500 (Invitrogen), mouse anti-Hts at 1:20 (1B1, DSHB), mouse anti-Myc at 1:250 (9E10, DSHB), and rabbit anti-PH3 at 1:1000 (Upstate Biotechologies/ Millipore). Alexa 488-conjugated (Molecular Probes/Invitrogen), Cy3- and Cy5-conjugated Donkey anti-mouse, anti-rabbit, and anti-goat secondary antibodies were used at 1:250 to 1:500.

In situ RNA hybridization

Smurf anti-sense and sense probes were synthesized from the 2.1 kb genomic fragment of exon 5 using DIG RNA labeling kit (Sp6/T7) (Roche). The exon 5 DNA was amplified from *Oregon R* adult genomic DNA by the following pair of primers and cloned into *T*-easy vector (Promega): TGTCGCCGGATGACGATGAGCTTGTAC and CGGATCCACGCCTTCAATATCACCAAGC. For RNA in-situ hybridization, testes were fixed in 4% paraformadehyde for 20 min, followed by proteinase K treatment for 5 min and a post-fix in 4% paraformaldehyde for 20 min. Testes were prehybridized in hybridization buffer (HB) at 65 °C for 60 min, followed by hybridization with Dig-labeled RNA probe in HB at 65 °C for 12–16 h. Testes were then washed with HB/PBST in 4:1, 1:1 and 1:4 dilution for 60 min for each wash, followed by incubation with pre-absorbed anti-DIG-AP antibody (1:2000) at 4 °C for 12–16 h. Testes were washed extensively with PBST for 20 min for six times before adding the NBT/X-Phosphate staining solution. After color reaction was stopped, testes were de-stained with 100% EtOH and EtOH/methyl salicylate and mounted on slide with 30–50 μl GMM (Canada balsam dissolved in methyl salicylate).

RT-PCR—RNA was extracted from 90 pairs of adult testes by TRIzol (Invitrogen). RT-PCR was performed by Onestep RT-PCR system (QIAGEN) for 25 cycles with the following primers:

Smurf: 5′-CGTCGCAATGGTACACACAAAGTTC-3′ and 5′-TATCTTCCGAGGAGTCATCTTCCGA-3′

*actin*5C: 5′-AGCAGTCGTCTAATCCAGAGAC-3′ and 5′-ATACATGGCGGGTGTGTTGAAG-3′.

Antibody generation, purification and Western blot analysis

Rabbit polyclonal antiserum was raised to His^6-Smurf a.a.211–538 recombinant protein, and antibody purification was performed using nitrocellulose membranes blotted with GST-Smurf a.a. 211–538 protein. For immunostaining of testes, antibody was pre-absorbed with 15–20 pairs of w^{1118} or $Smurf^{15C}/Df7149$ adult testes. For Western blot analysis, protein extracts were made from 20 pairs of 0–1 day adult testes.

Live cyst dissection

Adult testes were dissected in TB1 (15 mM potassium phosphate, pH 6.7, 80 mM KCl, 16 mM NaCl, 5 mM MgCl2, and 1% PEG 6000), and a single testis was moved to a clean slide with 27 μl TB1. To peel open the testes, the middle of the testis was held with one pair of forceps and the other pair of forceps was used to peel the testis sheath from the holding site. Most of cysts including spermatocyte cysts would be released. A coverslip was gently placed on the samples, and TB1 was removed by a kimwipe until the cysts was one-cell-layer thick (Insco et al., 2009).

Measurement of testis surface area

Adult testes were dissected in 1 × PBS. Immediately after dissecting, one test testis (with semi-transparent sheath) and one Oregon-R testis (with yellow sheath) were moved to the same slide with 50 μl 1 × PBS, and a cover slip was placed on the samples very gently. Four small 0.8 mm-thick stickers were placed between the slide and the cover slips to prevent uneven strain from the cover slip. The image of each pair of testes was taken at once (10 × objective). Surface area was determined by ImageJ, and normalized to the surface area of the Oregon-R testis mounted on the same slide.

Counting the germline stem cell number

GSCs were identified as Vasa-positive cells that attach to FasIII-or Arm-positive hub cells localized at the anterior apex (Inaba et al., 2011). To count the number of GSCs, *Z*-stacks of confocal images at 1–2 μm intervals were obtained through the depth of the hub.

Staging of developing Drosophila

Larvae 0–24 h after hatching were collected as L1. L2 and L3 larvae were determined on the basis of size difference and anterior spiracle morphology (Bodenstein, 1950). L2 were chosen as the smaller larvae with clubbed anterior spiracles. Early L3 are chosen as large larvae within the food with branched spiracles where all the braches were still attached to each other. Late L3 were chosen as the wandering larvae crawling on the tube wall, with branched spiracles where each branch was separated from the others. All puape were collected within 4 h after puparium formation (APF). All adults are 0- to 1-day adults.

Heat shock conditions

For generating *Smurf*^{15C} clones, larvae were incubated at 37 °C for 1 h at day 3 and 4 after starting cultures. For *hs-bam* experiment, larvae were incubated at 37 °C for 1 h at day-7, day-8 and day-9, and testes were dissected at day-12.

Fluorescence intensity quantification

The samples for comparison of fluorescence intensity were processed in parallel. Confocal images were obtained with a Zeiss LSM 510 Meta microscope at a fixed detection setting. *Z*-stacks of confocal images at 1–2 μm intervals were obtained for each testis. The mean fluorescent intensity in each cell was measured with ImageJ software in single confocal sections that scanned through the center of nucleus. Germ cells located at the periphery of mounted testes where the whole cells (whole circular anti-Vasapositive area) are on the different confocal section were not used for quantification. For each cell, all confocal images in different channels were taken in a single confocal session. The whole nuclear or cytoplasmic area (defined by Vasa-negative and Vasapositive region, respectively) was selected by Freehand tool in ImageJ for quantification. The α-pMad intensity for each GSC was determined after subtraction of a background value in a neighboring region of testis that was both Vasa-negative and pMadnegative. The α-pMad intensity for each mature cyst cell was obtained after subtraction of a background value in a neighboring region of testis that was pMad-negative. For comparison of α-pMad intensities between different genotypes at different developmental stages, the intensity for each cell was normalized to the average α-pMad intensity of 20 posterior terminal epithelial cells that are constantly positive for α-pMad staining. For comparison of α-pMad intensity between *Smurf* mutant and *myc-Smurf* rescue testes, testes were stained in the same reaction tube. In this set of experiment, all staining intensities including α-Myc and α-pMad were normalized to the mean α-Vasa fluorescence in the same cells. For the relative α-DSmurf intensity, mean cytoplasmic fluorescence of each wild-type GSC and spermatocyte was normalized to the mean α-Vasa fluorescence in the same cells. For the relative α-Bam intensity in 4-cell cysts, the average fluorescence in the cytoplasm of the four TA cells was determined after subtracting an average background value in spermatocytes in the same testes, followed by normalization by the average α-Vasa fluorescence in the same four TA cells. Samples with too low or too high α-Vasa staining intensity were not used for quantification. The mean α-GFP immunostaining intensity of Stg-GFP in each cyst was determined after subtracting a background value in the hub.

Plasmid construction

The full-length *Smurf* coding sequence was amplified from EST clone LD06566 by PCR. *Smurf* coding sequence with an N-terminal *myc* tag sequence was cloned into pUAST to generate *pUAST-myc-Smurf*. The C1029A substitution of Smurf was generated using QuikChange™ kit (Stratagene). The *Smurf* 1.4-kb *cis*-regulatory fragment, including the 310-bp upstream region and the first two exons (2R: 13,480,000–13,481,421), was amplified from *Oregon-R* genomic DNA by PCR and cloned into *pGreen Pelican* (Barolo et al., 2000) to generate *1.4-GFP*.

Results

Response to BMP signaling in GSCs is downregulated during development by Smurf

Analysis of α-pMad staining patterns in larval and pupal testes indicated that the level of responses to BMP signaling in germ cells normally falls as testes develop from larval to adult stage. In the first 4 h (0–4 h) after hatching of embryos to larvae, a few α-pMad positive cells were occasionally detected in early germ cells (Supplementary Fig. S1A and A′). Starting from 4 h after hatching, pMad was consistently detected in anteriorly localized germ cells (Fig. S1B and B). This expression pattern persisted throughout the mid first larval instar (L1) until 16 h after hatching (Fig. 1A and A′). pMad expression was restricted more anteriorly during 16–20 h after hatching, resolving to the hub-proximal cells including all GSCs and a few germ cells located nearby by the end of the L1 (Supplementary Fig. 1C and C′). pMad was still detected in hub-proximal germ cells in second instar (L2) and the feeding third instar (early L3; EL3) larval testes (Fig. 1B, B′ and C, C′). In the third instar wandering larvae (late L3; LL3), however, pMad was only detected in the GSCs and α-pMad staining levels were markedly decreased (Fig. 1D and D′). pMad levels in GSCs were even further reduced in 0–4 h after puparium formation (APF) testes (Fig. 1E and E′), and α-pMad staining was almost undetectable in testes from 0 to 1 day adults (Fig. 1F and F′).

The decrease in pMad levels in GSCs during development requires function of the E3 ligase Smurf. *Smurf*^{15C} is a hobo-element insertion allele that presumably encodes a truncated protein lacking the carboxyl-terminal HECT domain (Podos et al., 2001). *Df(2R)Exel7149* is the smallest deletion line available from Bloomington stock center that uncovers *Smurf*. While *Smurf* mRNA in *Smurf*^{15C}/*Df7149* adult testes was detected at a level comparable to that in *Df7149*/+ by RT-PCR (Fig. S2), antibody raised against *Drosophila* Smurf (anti-DSmurf) (see **Materials and methods**) detected no Smurf protein in *Smurf*^{15C}/*Df7149* testis extract by Western (Fig. 1M), indicating that the Smurf protein encoded by *Smurf*^{15C} is not stable. High levels of pMad signal were observed in GSCs and early spermatogonia in *Smurf*^{15C}/*Df7149* mutant testes from L1 to 0–1 day adult (Fig. 1G–L′), suggesting that Smurf activity normally downregulates pMad throughout development. Strong α-pMad signals were also present in *Smurf*^{15C}/*Smurf*^{15C} homozygous testes (Fig. 1N), but not in *Smurf*^{15C}/+ or *Df7149*/+ estes (data not shown). Quantification of α-pMad immunofluorescent intensity, normalized at a testis by testis basis to the α-pMad intensity in the posterior end terminal epithelial cells that are constantly positive for α-pMad antibody (arrows in Fig. 1O and O′) revealed that Smurf indeed is required for downregulation of pMad in GSCs from EL3 to early pupae. While the median value of the relative α-pMad intensity was drastically decreased from 0. 77 arbitrary units at EL3 (*N*=38) to 0.03 units at LL3 (*N*=39) and 0.06 units at early pupa (*N*=41) (Fig. 1P), median α-pMad intensity in *Smurf*^{15C}/*Df7149* GSCs remained relatively constant, with 0.91 units at EL3 (*N*=37), 1.11 units at LL3 (*N*=41) and 1.03 units at early pupa (*N*=41) (Fig. 1P). Further examination of the spatial distribution of pMad in 0–1 day *Smurf*^{15C}/*Df7149* testes revealed anti-pMad signal in GSCs, goniablasts and two-cell stage TA cells (Fig. 3B). Together, these results demonstrated that Smurf is required for spatial and temporal downregulation of pMad levels in GSCs and early germ cells during testis development.

Analysis of expression of *Dad-LacZ*, a reporter of transcriptional activation downstream of BMP signaling, also indicated that Smurf is essential for a similar decline in BMP signaling activity during testis maturation from larval to adult stages. β-Galactosidase expressed from *Dad-LacZ* was detected in GSCs and early germ cells in some L1 testes and all testes from L2 to early pupal stages (Fig. 2A–E′). Strong down-regulation of *Dad-LacZ* in the early germ cells occurred between the pupal and adult stage, perhaps in part due to perdurance of β-galactosidase (Lu et al., 2012). Under the same experimental conditions used for larval and pupal gonads, expression of β-galactosidase from *Dad-LacZ* in GSCs and early germ cells from wild-type 0–1 day adult testes was barely detected (Fig. 2F and F′). In $Smurf^{15C}$/*Df7149* testes, expression of *Dad-lacZ* was also elevated in 0–1 day adult GSCs and early germ cells to a level comparable to that in wild-type larval and pupal testes (Fig. 2G and G′).

Smurf acts via an E3 ligase-dependent mechanism to cell autonomously down-regulate pMad levels in germ cells

Clonal analysis revealed that action of *Smurf* is required cell autonomously in GSCs and early germ cells to downregulate response to BMP signaling as testes develop. When clones of germ cells homozygous mutant for $Smurf^{15C}$ were generated in the larval stage, pMad levels increased dramatically in $Smurf^{15C}$/$Smurf^{15C}$ GSCs, goniablasts and 2-cell stage spermatogonia in 0–1 day adult testes (Fig. 3A–A″), similar to the spatial distribution of pMad in 0–1 day $Smurf^{15C}$/*Df7149* testes (Fig. 3B). The downregulation of the response to BMP signaling required the E3 ligase activity of Smurf. Expression of *myc-Smurf* in GSCs and spermatogonia under control of *nos-Gal4* completely suppressed pMad accumulation in $Smurf^{15C}$/*Df7149* testes (Fig. 3C). In contrast, a mutant Smurf protein with a cysteine-to-alanine substitution (SmurfC1029A) that disrupts the E3 ligase activity (Liang et al., 2003) failed to suppress pMad accumulation in early germ cells (Fig. 3D).

In *Drosophila* ovaries, Smurf cooperates with the serine/threonine kinase Fused (Fu) to degrade the BMP signaling receptor Tkv in cystoblasts (Cbs) (Xia et al., 2010), allowing differentiation of Cbs. Examination and quantification of α-pMad immunofluorescence in *fu* null mutant fu^{mH63}/*Y* testes revealed that the α-pMad intensity in GSCs was also temporally downregulated from EL3 (median value 1.13 units) to early pupa (median value 0.14 units) (Figs. 3E, F, and S3A), indicating that Fu is not essential for Smurf-mediated suppression of BMP signaling activity in GSCs.

α-pMad immunofluoresence and *Dad-lacZ* expression was also constantly detected in mature somatic cyst cells that surround the differentiating spermatocytes from larva to adult (Figs. S4A, B and 3A′ and Fig. 2A–F′). Quantification of α-pMad immunofluoresence in the somatic cells surrounding the germ cells at the transition from proliferation to differentiation (arrows in Fig. S4A and B) showed mild reduction of pMad levels from EL3 (median value 0.71 units) to pupae (median value 0.33 units) in w^{1118} testes (Fig. S4C). Decrease in α-pMad intensity in somatic cyst cells was observed in $Smurf^{15C}$/*Df7149* testes form EL3 to early pupae (Fig. S4C), suggesting that the action of Smurf to downregulate BMP signaling is specific to germ cells.

Smurf limits stem cell number during gonad metamorphosis in the pupal stage

In wild-type, the average number of GSCs around the hub per testes decreases during development, correlating with the decrease of pMad levels in GSCs. In w^{1118} early pupae 0–4 h APF, testes had an average of 10.4 ± 2.2 GSCs (Fig. 4A). In newly eclosed w^{1118} adults 0- to 1-days old, GSC number was significantly decreased to 8.7 ± 1.4 ($p<0.001$) (Fig. 4A). Reduction in GSC numbers from early pupa to adult was also observed in the testes from $Smurf^{15C}$/+ (11.2 ± 1.8 to 8.6 ± 1.2, $p<0.001$) and *Df7149*/+ (11 ± 1.9 to 9.6 ± 1.5, $p<0.01$) (Fig. 4A). The decrease in GSC number was not accompanied by a decrease in hub size; the hub diameter remained comparable between 0–4 h APF pupal gonads and 0- to 1-day adult testes in w^{1118} and *Smurf* heterozygous mutant flies ($p>0.05$, Fig. 4B).

Block in pMad downregulation in *Smurf* mutant testes, strikingly, correlated with maintenance of the higher GSC number. In $Smurf^{15C}$/*Df7149* mutants, GSC number in 0- to 1-day adult testes averaged 11.4 ± 1.9, comparable to 10.9 ± 1.9 GSCs in early pupal testes ($p>0.05$) (Fig. 4A). Maintenance of GSC number from early pupa to adult was also observed in $Smurf^{15C}$/$Smurf^{15C}$ testes (8.5 ± 1.6 to 7.9 ± 1.9, $p>0.05$) (Fig. 4A), although $Smurf^{15C}$/$Smurf^{15C}$ pupal testes had fewer GSCs than the other pupal testes examined (Fig. 4A). We speculated that it might be due to other genetic alterations in $Smurf^{15C}$ genetic background that affect germ cell proliferation, since the $Smurf^{15C}$ mutant clones exhibited a much stronger spermatogonia overporliferation phenotype compared to $Smurf^{15C}$/$Smurf^{15C}$ testes (see below, Fig. 5D and E).

The increase in GSC number in $Smurf^{15C}$/*Df7149* adult was likely due to the higher pMad levels in $Smurf^{15C}$/*Df7149*. GSC number in $Smurf^{15C}$/*Df7149* testes with one null allele mad^{12} was significantly decreased to 9.6 ± 1.9 ($p<0.001$) (red bars in columns 4 and 5 in Fig. 4A). While GSC numbers varied in adults (red bars in Fig. 4A), there was no significant difference in the early pupal GSC numbers among testes from different genotypes except for $Smurf^{15C}$/ $Smurf^{15C}$ ($p>0.05$) (blue bars in Fig. 4A). In contrast to the higher GSC number in $Smurf^{15C}$/*Df7149* adults, no significant difference in hub diameter was observed among the different genotypes tested (Fig. 4B). Taken together with the pMad patterns in larval and pupal testes, we propose that action of Smurf reduces the number of GSCs in adult testes by downregulating pMad to a very low level during gonad metamorphosis in the pupal stage.

Downregulation of pMad by Smurf influences the number of TA divisions

In addition to regulating GSC number, Smurf acts cell autonomously in germ cells to restrict the number of spermatogonia transit amplifying divisions. In wild-type LL3 testes, the final round of mitosis occurred in 8-cell spermatogonia (data not shown). However, spermatogonial cysts with >8 cells undergoing mitosis in synchrony were detected in $Smurf^{15C}$/*Df7149* LL3 testes (Fig. 5A), suggesting that some TA cysts underwent at least one extra round of cell division in developing testes from $Smurf^{15C}$/*Df7149* mutant larvae. Counts of cell number in individual spermatocyte cysts in testes from newly eclosed adults confirmed that a significant fraction of TA cell cysts underwent one extra round of division in *Smurf* mutant testes. In testes from $Smurf^{15C}$/+ or *Df7149*/+males, nearly all (98.2% and 99.8%, respectively) of the spermatocyte cysts scored contained 16 cells, indicating four rounds of TA division (Fig. S5A, lanes 1 and 2 in Fig. 5D). In $Smurf^{15C}$/*Df7149* 0–1 day

adult testes, in contrast, 25.8% of the spermatocyte cysts scored contained 32 cells (asterisks in Fig. S5B, and lane 4 in Fig. 5D). Cysts containing 32 spermatocytes appeared to undergo meiosis correctly and progress into spermatid differentiation; the percentage of the early spermatid cysts with 128 cells observed (33%) (Fig. 5C) was comparable to that of the 32-spermatocyte cysts (25.8%) in *Smurf*^{15C}/*Df7149* testes. The requirement for Smurf for the normal number of division was cell autonomous, as the 32-cell phenotype in *Smurf*^{15C}/*Df7149* testes was almost completely rescued by expression of *UAS-myc-Smurf* in early germ cells under control of *nos-Gal4* (lane 10 in Fig. 5D). Also, 30% of the *Smurf*^{15C} mutant clone cysts had 32 spermatocytes and all *Smurf*^{15C}/+ spermatocyte cysts had 16 cells (Fig. 5E). Surprisingly, 95% of the spermatocyte cysts in *Smurf*^{15C}/*Smurf*^{15C} testes had 16-cells (lane 3 in Fig. 5D). This low percentage of TA overproliferation likely reflected additional genetic alternations in the *Smurf*^{15C} homozygous background.

The overproliferation of TA cysts in *Smurf* mutant testes likely represents a consequence of the elevated pMad in the mutant early germ cells, as the percentage of 32-spermatocyte cysts in *Smurf*^{15C}/*Df7149* was significantly reduced in a genetic background mutant for one copy of *mad*$^{1–2}$ (from 25.8% to 5.2%) or *mad*^{12} (from 25.8% to 9.0%) (Fig. 5D). In contrast, the number of TA division was not sensitive to defects in *fu*. Because null *fu*^{mH63}/*Y* mutants failed to survive to adulthood, the numbers of spermatocytes in single cysts were examined in testes from adult male flies carrying *fu*^{50}, a viable allele that exhibits the strongest germline tumor phenotype in ovary that is resulting from hyperactivation of BMP signaling in cystoblasts (Narbonne-Reveau et al., 2006). Consistent with our finding that *fu* was not essential for downregulation of pMad in early germ cells during testis development, 32-cell cysts were not observed in *fu*^{50} testes (lane 7 in Fig. 5D). The percentages of 32-cell cysts were also low in adult testes from two other viable *fu* mutants: 2.9% (*N*=68) in hemizygous mutants of *fu*^{54} that encodes a truncated protein having only the N-terminal 80 amino acids, and 3.2% (*N*=158) in hemizygous mutants of the hypomorphic *fu*^{52} (Fig. S3B).

Higher Cdc25 level is essential for TA cell overproliferation in developing Smurf mutant testes

Previous genetic studies suggest that accumulation of Bam protein sets the timing of the switch from proliferation to differentiation (Insco et al., 2009). In wild-type testes, Bam expression was first detected in 4-cell cysts, reaching peak levels in 8-cell cysts and decreasing in early 16-cell cysts (Insco et al., 2009). Loss of *Smurf* function may affect the number of rounds of TA division by delaying onset of Bam protein expression. Comparison of α-Bam immunofluorescent intensities in 4-cell cysts from heat shock-induced *Smurf*^{15C}/*Smurf*^{15C} clones versus neighboring *Smurf*^{15C}/+ heterozygous 4-cell cysts indicated that loss of Smurf in early germ cells delayed onset of Bam expression in 4-cell cysts. To compare Bam levels among cysts from different testes, the average α-Bam staining intensities in the four TA cells were normalized to the average co-stained α-Vasa intensities in the same cysts. In the *Smurf*^{15C}/+ 4-cell cysts, a variety of α-Bam intensities from low (below 33% of the maximal α-Bam intensity in 4-cell cysts of +/+ control testes), medium (34–66%) to high (67–100%) were observed in 6%, 82% and 12% of cysts, respectively (Fig. 5F). In *Smurf*^{15C} clones, the percentage of low-Bam cysts was increased to 39% (Fig. 5F, $p<0.05$). The mean α-Bam intensity of 4- cell cysts was also significantly decreased in the *Smurf*^{15C}/

Smurf^{15C} clones (0.38 ± 0.13, *N*=18) compared to the *Smurf*^{15C}/+ (0.51 ± 0.14, *N*=17) ($p<0.05$) (Fig. 5F)

Although Smurf was required for timely onset of Bam expression in 4-cell cysts, Bam levels may not be the only target of Smurf important for the proper number of TA divisions. Forced expression of Bam in *Smurf*^{15C}/*Df7149* larvae under control of a heat shock promoter (*hs-bam*) failed to rescue the overproliferation phenotype; 32 cells were observed in 23.5% spermatocyte cysts and there were no 8-cell cysts (Fig. 5G), which was comparable to *Smurf*^{15C}/*Df7149* mutants that did not carry the *hs-Bam* transgene but were subjected to the same heat shock treatment (Fig. 5G). In contrast, in sibling control testes carrying *hs-bam* in *Smurf*^{15C}/+ background, heat shock treatment during pupal stage promoted premature termination of TA mitosis; 26.6% of spermatocyte cysts had only 8 cells and none of them had 32 cells in adult testes (Fig. 5G).

TA cell overproliferation can also be caused by higher cell cycling activity (Insco et al., 2009). Forced expression of *String* (*stg*), the *Drosophila* Cdc25 homologue critical for G2-M transition, was sufficient to drive extra rounds of mitosis in TA cells (Insco et al., 2009) (Fig. 5H). In contrast, overexpression of other critical G1/S or G2/M cell cycle regulators such as CycE, CycA or CyB failed to trigger overproliferation (Fig. 5H), indicating that Cdc25 plays an important role and may be rate limiting in determining the number of TA mitoses. To test whether Smurf regulates TA division through *stg*, Stg expression was examined by the GFP protein trap line *Stg-GFP* that is regulated under *stg* native promoter. Stg-GFP expression, detected by α-GFP immunofluorescence, was at the background level in 8- and 16-cell cysts in heterozygous sibling *Smurf*^{15C}/+ or *Df7149*/+ LL3 testes (Fig. 5I and K). In *Smurf*^{15C}/*Df7149* LL3 testes, α-GPF staining intensities in 8- and 16-cell cysts were markedly increased (Fig. 5J and K). Inactivation of one copy of *stg* in *Smurf*^{15C}/*Df7149* strongly suppressed the 32-cell spermatocyte cyst phenotype from 36% (*N*=151) to 10.3% (*N*=136) (Figs. 5H, $p<0.01$). Together, these results suggest that negative regulation of Cdc25 expression is essential for Smurf to restrict TA division during testis development.

Downregulation of pMad is important for Smurf-mediated testis size control

Under the dissecting microscope, the most prominent feature of *Smurf* mutant adult testes was the change in size. In both *Smurf*^{15C}/*Smurf*^{15C} and *Smurf*^{15C}/*Df7149* mutant animals, testes appeared larger compared to the wild type *w*^{1118} testes (Fig. 6A–C). Quantification of the adult testis surface area, which was normalized to the surface area of the *Oregon-R* testes mounted on the same slide (Fig. 6G), showed that the relative mean value of *Smurf*^{15C}/*Df7149* testis surface area was 1.55-fold, which was significant higher than the 0.9-fold of the *w*^{1118} testes ($p<0.001$) (Fig. 6H). Likewise, the relative mean value of *Smurf*^{15C}/*Smurf*^{15C} testis surface area was 1.48-fold (Fig. 6H). Despite the size increase, the general morphology and organization of *Smurf* mutant testes were normal; the DNA-bright undifferentiated small germ cells were found only at the testis apex and the sperm with compacted and elongated nuclei were present mostly at the basal end of the testis, similar to that in *w*^{1118} testes (Fig. 6D–F), indicating that Smurf regulated growth without affecting testis organization.

The requirement for Smurf function to regulate testis size appeared to involve downregulation of the response to BMP signaling, as reduction of *mad* gene activity also decreased testis size in *Smurf* mutants. The relative mean surface area was significantly reduced from 1.55-fold of $Smurf^{15C}/Df7149$ testes to 1.3-fold or 1.34-fold of $Smurf^{15C}/Df7149$ testes carrying one copy of hypomorphic allele mad^{1-2} or one copy of null allele mad^{12}, respectively ($p<0.001$) (Fig. 6H).

Smurf is expressed at very low levels in GSCs and spermatogonia

In situ hybridization of 0–1 day adult testes revealed that *Smurf* mRNA was expressed at almost undetectable levels in GSCs and spermatogonia (black arrow in inset in Fig. 7A). *Smurf* mRNA robustly upregulated at the spermatogonia to spermatocyte transition (yellow arrow in inset in Fig. 7A). No signals were detected with *Smurf* sense probe (Fig. 7B). The high-level *Smurf* mRNA in germ cells was not observed in *bam* mutant testes, which do have TA cells but not spermatocytes (Fig. 7D). The *Smurf* mRNA expression in testes was controlled, at least in part, by *cis*-regulatory sequences located from 310 bp upstream of the transcription start site to 64 bp after the ATG start codon, since a *Smurf*-GFP reporter gene carrying 1.4 kb sequences from −310 to 1000 bp of the *Smurf* gene (Fig. 7G) activated GFP expression in a very similar pattern as the *Smurf* mRNA (Fig. 7E–E″). The low-level α-GFP immunofluoresence in spermatogonia is specific to *1.4-GFP* since no GFP expression was detected in w^{1118} control testes (Supplementary Fig. S6B and B′). Patterns of *Smurf* mRNA and the *1.4-GFP* reporter expression in developing L3 and early pupal testes were very similar to those in 0–1 day adults, with low expression in spermatogonia and abrupt up-regulation in cells at the transition from spermatonia to spermatocyte (Fig. 7C, F and data not shown).

Despite the Smurf-dependent dramatic decline in pMad levels in GSCs from EL3 to early pupal testes, immunofluorescence analysis indicated that Smurf might be expressed at a constant level in germline stem cells across larval to pupal stages. Although the anti-DSmurf antibody stained nuclei nonspecifically in $Smurf^{15C}/Df7149$ EL3 and early pupal testes (Fig. 7H, I and area enclosed by a yellow dotted line in inset in Fig. 7M), Smurf-specific immunofluorescent signals were strongly detected in the cytoplasm of germ cells entering spermatocyte differentiation (Fig. 7J and K). Low-level α-Smurf immunofluoresence was also detected in the w^{1118} GSCs as well as spermatogonia (Fig. 7J and K) in the cytoplasm (region between a white line and a yellow dotted line in Fig. 7L). In addition, anti-DSmurf immunofluoresence was detected in hub cells and early cyst cells (Fig. 7J and K) although Smurf was not required for downregulating pMad levels in the somatic cells (Fig. S4C and data not shown). Quantification of the cytoplasmic anti-DSmurf staining intensity, which was normalized to the co-stained α-Vasa intensity in the GSC cytoplasm, showed that the low-level anti-DSmurf staining intensity in w^{1118} GSCs was significantly higher than in the $Smurf^{15C}/Df7149$ GSCs (Fig.7N). However, no significant difference was found in the levels of anti- DSmurf immunflurorescence in GSCs of EL3 versus early pupae (Fig. 7N), suggesting that Smurf may be expressed at a constant level in germline stem cells across larval to pupal stages. No difference was observed for the α-DSmurf intensities in spermatocytes between EL3 and early pupal testes (Fig. 7O).

Smurf promotes differential BMP signaling attenuation in a stagedependent but concentration-independent manner

The further test the idea that developmental regulation of pMad is independent of the levels of Smurf expression, Myc- Smurf was expressed in *Smurf*^{15C}/*Df7149* early germ cells including GSCs and spermatogonia under control of *nos-Gal4*. Larvae were incubated at 18 °C to reduce GAL4/UAS efficiency to avoid excessive overexpression. Due to the variability of *nos-Gal4* driven expression (Inaba et al., 2010), Myc-Smurf levels were not uniform among individual GSCs (Fig. 8A, A′, B and B′). To compare pMad levels in GSCs expressing similar amounts of Smurf, the GSCs were sorted into three groups based on intensity of α-Myc immunofluorescence: Smurf-low (lowest 33% among all GSCs in *nos* > *Smurf* EL3, LL3 and pupal testes), Smurf-medium (in-between), and Smurf-high (highest 33%). Myc-Smurf intensity in each group was comparable between EL3, LL3 and early pupae (0.22, 0.20, and 0.18 arbitrary units for Smurf-low; 0.63, 0.66, and 0.52 units for Smurf-medium; 1.34, 1.48, and 2.04 units for Smurf-high). In the Smurf-low EL3 GSCs, α-pMad intensity was reduced to 25% of that detected in *Smurf*^{15C}/*Df7149* EL3 GSCs (Fig. 8A and C), indicating that Myc-Smurf partially suppressed pMad accumulation in EL3 GSCs. Strikingly, pMad accumulation was completely suppressed by Myc-Smurf in Smurf-low early pupal GSCs (Fig. 8A and C). Likewise, pMad accumulation was also suppressed in GSCs from pupal compared to EL3 testes, within the Smurf-medium class and within the Smurf-high class as well (Fig. 8A and C), indicating that downregulation of pMad in pupal compared to EL3 larval GSCs correlated well with developmental stage. Further comparison of α-pMad intensity among Smurf-low, medium, and high GSCs found that pMad levels were not further reduced in Smurf-high GSCs compared to Smurf-low and Smurf-medium GSCs at the same developmental stage (Fig. 8C). Thus, while the lowest level of Smurf appeared to be sufficient for downregulation of pMad in pupal GSCs, excess Smurf protein did not significantly further enhance BMP signaling attenuation in GSCs.

Conclusions and discussion

BMP signaling is central for regulation of self-renewal and proliferation of various types of stem cells from *Drosophila* to mammals (Zhang and Li, 2005). In the *Drosophila* female germline, response to BMP signaling is activated in stem cells at a relatively constant level, and it is critical for adult stem cell maintenance. In the *Drosophila* male germline, in contrast, we found that BMP signaling is dynamically regulated in stem cells and early germ cells in the developing testes, being spatially restricted and temporally downregulated during larval and pupal development. The attenuation of BMP signaling requires action of the ubiquitin E3 ligase Smurf and is important in limiting stem cell number, spermatogonia cell proliferation and, consequently, testis size. Analysis of Smurf protein levels in the larval versus pupal GSCs and results from rescue experiments support the hypothesis that the competence of Smurf protein to suppress BMP signaling may be differentially regulated in earlier L3 larvae versus pupal and adult stage.

Dynamic BMP signaling activation in developing testes

GSCs are established from primordial germ cells and initiate asymmetric division around embryonic stage mid 17. Several hours later, around 28 h after egg laying, Bam protein

starts to accumulate in the posterior germ cells to initiate differentiation (Sheng et al., 2009). Our results showed that the high levels of pMad expression in germ cells were not detected until 4 h after hatching, coinciding with the onset of Bam expression. Thus, response to BMP appeared low during or immediately after GSC establishment, but increased in anterior germ cells at a time when posterior germ cells begin to enter differentiation. Recent studies of *Drosophila* ovarian development revealed that initiation of both germ cell and niche differentiation is coordinated in third instar larvae by hormonal signaling in somatic cells, so that as germ cell differentiation programs initiate, future stem cells are protected from differentiating (Gancz et al., 2011). It remains to be seen whether the onset of both BMP signaling activation and germ cell differentiation is coordinated by a common upstream signaling in early testis development as well.

From late L1 to EL3, high levels of pMad expression were restricted to the neighborhood of the hub, including GSCs and a few other early germ cells adjacent to GSCs, reminiscent the restriction of BMP signaling pathway activation to GSCs in adult ovary, and suggests that short-range BMP signaling from the niche might be important for the continuous pMad expression in GSCs in L2 and L3 larvae. Several mechanisms have been shown to contribute to restricted BMP signaling activation within the niche, such as localized activation of Tkv receptor at the adherents junctions at the hub–GSC interface (Michel et al., 2011), nichespecific expression of BMP ligands (Shivdasani and Ingham, 2003) and BMP signaling co-receptors Dally and Dally-like glypicans (Hayashi et al., 2009), and action of extracellular matrix proteins to prevent BMP ligand diffusion (Wang et al., 2008). It is very likely that at least one of these mechanisms is activated as early as in the L1/L2 transition to restrict BMP signaling activation to hub-proximal cells in L2 larval testes.

Regulation of TA proliferation and testis growth by BMP signaling attenuation

Previous studies have shown that reduction in the numbers of early germ cells, for example by overexpressing Bam under the control of *nos-Gal4*, resulted in reduced testis size (Bunt and Hime, 2004; Schulz et al., 2004; Shivdasani and Ingham, 2003). Our results suggest that action of Smurf controls testis size, at least in part, through limiting the number of TA mitosis. In previous studies, elevated BMP signaling that promotes continuous TA division was achieved by forced overexpression of ligands or the constitutively active receptors in all early germ cells. In these testes, TA cells fail to enter spermatocyte differentiation, leading to small testes full of overproliferated spermatogonia. In contrast, pMad upregulation in *Smurf* mutant testes resulted in larger testis size, accompanied by often delayed but successful onset of spermatocyte differentiation. The opposite effect on testis organ size likely can be explained by the difference in spatial regulation of BMP pathway activation. While overexpression of ligand or constitutively active receptors resulted in constitutive activation of BMP signaling in all spermatogonia (Schulz et al., 2004), loss of *Smurf* led to up-regulation of BMP signaling activity only in GSCs, goniablasts and two-cell stage TA cells. It seems that the restricted activation of BMP signaling in the very early germ cells only transiently delayed onset of Bam expression, allowing differentiation to proceed once germ cells had moved away from the testis tip. The restricted activation of BMP signaling to up to two-cell cysts in *Smurf* mutants could result from short-range signaling of BMP from the apical niche or the early cyst cells. Alternatively, additional negative regulators might act

in more mature TA cysts to further suppress the BMP responses. pMad expression was still restricted to the neighborhood of the hub in *Smurf bam* double mutant adult testes (unpublished results), suggesting that downregulation of BMP pathway activation in anteriorly localized early germ cells in the adult testes does not depend on activity of Bam. Together, our results reveal that precise control of spatial activation of the BMP pathway plays versatile roles in regulation of proliferation versus differentiation in male gonad development.

Previous studies have shown that Bam is important to determine the numbers of TA mitosis (Insco et al., 2009) and TA cells continuously proliferate in double mutants for *put* (the type II receptor) and *bam* (Shivdasani and Ingham, 2003), indicating that the BMP pathway, when is in normal or reduced activity in wildtype and *put* mutant testes, respectively, regulates TA proliferation primarily through Bam. Our results show that TA overproliferation was suppressed by reduced *mad* and *stg* activity but not by elevated Bam expression in *Smurf* mutants, suggesting a model that high-level BMP signaling activity in early germ cells might have additional function that promotes Cdc25 expression and G2/M progression of TA cells downstream or parallel to Bam. In addition to TA cells in male germline, mitogenic activity of the BMP pathway is observed in imaginal disc growth and clonal expansion of ovarian primodial germ cells (Zhu and Xie, 2003), suggesting a conserved role of BMP signaling in regulation of cell proliferation in different *Drosophila* tissues.

Regulation of Smurf expression and activity in developing testes

Our rescue experiments revealed that even low levels of Smurf protein expressed in early germ cells were sufficient to cell autonomously restore pMad downregulation in germ cells in pupal testes, consistent with the finding that endogenous Smurf mRNA and protein were expressed at very low levels in early germ cells. The observation that higher levels of Smurf protein did not further enhance pMad downregulation, suggests that, while Smurf is required for downregulation of pMad in GSCs, the developmental difference in pMad levels in early larvae versus pupal or adult GSCs is likely not regulated at the level of Smurf expression. One possibility is that it is the competence of Smurf for BMP signaling attenuation that changes during development. Studies have shown that Smurf E3 ligase activity can be modulated through posttranslational modification or protein–protein interaction. Phosphorylation of mammalian Smurf1 at Thr^{306} by protein kinase A changes Smurf substrate preference during axon development (Cheng et al., 2011). The E3 ligase activity of HECT domain proteins Smurf2 and Itch is autoinhibited by intramolecular binding (Gallagher et al., 2006; Wiesner et al., 2007), and phosphorylation disrupts the autoinhibitory binding and greatly enhances the E3 ligase activity (Gallagher et al., 2006). Several Smurf interacting proteins, such as LMP-1, Synaptopodin, Fu and CKIP-1, suppress or enhance Smurf E3 ligase activity on particular substrates by modulating Smurf binding affinity to these targets (Asanuma et al., 2006; Lu et al., 2008; Sangadala et al., 2006; Xia et al., 2010). Conversely, modification of the substrates can also determine the competence of Smurf for protein degradation. Phosphorylation of Tkv by the Ser/Thr kinase Fu is important for Smurfmediated Tkv degradation in cystoblasts in the *Drosophila* ovary (Xia et al., 2010). However, a different mechanism likely acts in male GSCs to mediate the competence

of Smurf for downregulation of the BMP pathway since Fu is not important for pMad downregulation in *Drosophila* testes. The differential BMP signaling attenuation in GSCs appeared to not be mediated by ecdysone signaling in germ cells, since inactivation of ecdysone receptors in early germ cells did not prevent pMad downregulation in pupal GSCs (Supplementary Fig. S7A and B).

Smurf expression was dramatically elevated in differentiating spermatocytes upon the transition of spermatogonia to spermatocytes. Interestingly, mouse Smurf1 and Smurf2 are also expressed in spermatogonia, spermatocytes and round spermatids in testes (Itman et al., 2011). It is unclear, however, what the functions of Smurf may be in germ cell differentiation, since morphologically 118 normal spermatids formed in *Smurf* mutant adult testes and *Smurf* mutant males were fertile.

Supplementary Material

Refer to Web version on PubMed Central for supplementary material.

Acknowledgments

We are grateful to Cheng-Ting Chien, Margaret Ho and Hwei-Jan Hsu for critical comments on this manuscript. We thank Dan Vasiliauskas, Susan Morton, Tom Jessell, Ed Laufer, Erika Matunis and Edwin L. Ferguson for providing antibodies and flies, Yi-Chin Wu for technical support, and Ching-Yi Chen for support for manuscript preparation. This study is supported by grants from National Science Council of Taiwan, Molecular Medicine Center of Chang Gung University, and Chang Gung Memorial Hospitals to H.P. and NIH RO1 GM080501 to M.T.F. who also acknowledges the Reed-Hodgson Professorship in Human Biology, which partially supported this work.

References

Asanuma K, Yanagida-Asanuma E, Faul C, Tomino Y, Kim K, Mundel P. Synaptopodin orchestrates actin organization and cell motility via regulation of RhoA signalling. Nat. Cell Biol. 2006; 8:485–491. [PubMed: 16622418]

Barolo S, Carver LA, Posakony JW. GFP and beta-galactosidase transformation vectors for promoter/enhancer analysis in Drosophila. BioTechniques. 2000; 29:726–732. [PubMed: 11056799]

Bodenstein D. The postembryonic development of Drosophila. Biol. Drosophila. 1950:275–367.

Bunt SM, Hime GR. Ectopic activation of Dpp signalling in the male Drosophila germline inhibits germ cell differentiation. Genesis. 2004; 39:84–93. [PubMed: 15170693]

Casanueva MO, Ferguson EL. Germline stem cell number in the Drosophila ovary is regulated by redundant mechanisms that control Dpp signaling. Development. 2004; 131:1881–1890. [PubMed: 15105369]

Chen D, McKearin D. Dpp signaling silences bam transcription directly to establish asymmetric divisions of germline stem cells. Curr. Biol. 2003a; 13:1786–1791. [PubMed: 14561403]

Chen D, McKearin DM. A discrete transcriptional silencer in the bam gene determines asymmetric division of the Drosophila germline stem cell. Development. 2003b; 130:1159–1170. [PubMed: 12571107]

Cheng PL, Lu H, Shelly M, Gao H, Poo MM. Phosphorylation of E3 ligase Smurf1 switches its substrate preference in support of axon development. Neuron. 2011; 69:231–243. [PubMed: 21262463]

Crickmore MA, Mann RA. Hox control of organ size by regulation of morphogen production and mobility. Science. 2006; 313:63–68. [PubMed: 16741075]

Davies EL, Fuller MT. Regulation of self-renewal and differentiation in adult stem cell lineages: lessons from the Drosophila male germ line. Cold Spring Harbor Symp. Quant. Biol. 2008; 73:137–145. [PubMed: 19329574]

Edgar BA, O'Farrell PH. Genetic control of cell division patterns in the Drosophila embryo. Cell. 1989; 57:177–187. [PubMed: 2702688]

Gallagher E, Gao M, Liu YC, Karin M. Activation of the E3 ubiquitin ligase Itch through a phosphorylation-induced conformational change. Proc. Natl. Acad. Sci. USA. 2006; 103:1717–1722. [PubMed: 16446428]

Gancz D, Lengil T, Gilboa L. Coordinated regulation of niche and stem cell precursors by hormonal signaling. PLoS Biol. 2011; 9:e1001202. [PubMed: 22131903]

Gonczy P, Matunis E, DiNardo S. bag-of-marbles and benign gonial cell neoplasm act in the germline to restrict proliferation during Drosophila spermatogenesis. Development. 1997; 124:4361–4371. [PubMed: 9334284]

Hayashi Y, Kobayashi S, Nakato H. Drosophila glypicans regulate the germline stem cell niche. J. Cell Biol. 2009; 187:473–480. [PubMed: 19948496]

Hu X, Cherbas L, Cherbas P. Transcription activation by the ecdysone receptor (EcR/USP): identification of activation functions. Mol. Endocrinol. 2003; 17:716–731. [PubMed: 12554759]

Inaba M, Yuan H, Salzmann V, Fuller MT, Yamashita YM. E-cadherin is required for centrosome and spindle orientation in Drosophila male germline stem cells. PloS One. 2010; 5:e12473. [PubMed: 20824213]

Inaba M, Yuan H, Yamashita YM. String (Cdc25) regulates stem cell maintenance, proliferation and aging in Drosophila testis. Development. 2011; 138:5079–5086. [PubMed: 22031544]

Insco ML, Leon A, Tam CH, McKearin DM, Fuller MT. Accumulation of a differentiation regulator specifies transit amplifying division number in an adult stem cell lineage. Proc. Natl. Acad. Sci. USA. 2009; 106:22311–22316. [PubMed: 20018708]

Itman C, Wong C, Whiley PA, Fernando D, Loveland KL. TGFbeta superfamily signaling regulators are differentially expressed in the developing and adult mouse testis. Spermatogenesis. 2011; 1:63–72. [PubMed: 21866277]

Kavsak P, Rasmussen RK, Causing CG, Bonni S, Zhu H, Thomsen GH, Wrana JL. Smad7 binds to Smurf2 to form an E3 ubiquitin ligase that targets the TGF receptor for degradation. Mol. cell. 2000; 6:1365–1375. [PubMed: 11163210]

Kawase E, Wong MD, Ding BC, Xie T. Gbb/Bmp signaling is essential for maintaining germline stem cells and for repressing bam transcription in the Drosophila testis. Development. 2004; 131:1365–1375. [PubMed: 14973292]

Leatherman JL, DiNardo S. Zfh-1 controls somatic stem cell self-renewal in the drosophila testis and nonautonomously influences germline stem cell self-renewal. Cell Stem Cell. 2008; 3:44–54. [PubMed: 18593558]

Leatherman JL, Dinardo S. Germline self-renewal requires cyst stem cells and stat regulates niche adhesion in Drosophila testes. Nat. Cell Biol. 2010; 12:806–811. [PubMed: 20622868]

Liang YY, Lin X, Liang M, Brunicardi FC, ten Dijke P, Chen Z, Choi KW, Feng XH. dSmurf selectively degrades decapentaplegic-activated MAD, and its overexpression disrupts imaginal disc development. J. Biol. Chem. 2003; 278:26307–26310. [PubMed: 12754252]

Lin X, Liang M, Feng XH. Smurf2 is a ubiquitin E3 ligase mediating proteasome-dependent degradation of Smad2 in transforming growth factor-beta signaling. J. Biol. Chem. 2000; 275:36818–36822. [PubMed: 11016919]

Lu K, Yin X, Weng T, Xi S, Li L, Xing G, Cheng X, Yang X, Zhang L, He F. Targeting WW domains linker of HECT-type ubiquitin ligase Smurf1 for activation by CKIP-1. Nat. Cell Biol. 2008; 10:994–1002. [PubMed: 18641638]

Lu W, Casanueva MO, Mahowald AP, Kato M, Lauterbach D, Ferguson EL. Niche-associated activation of rac promotes the asymmetric division of Drosophila female germline stem cells. PLoS Biol. 2012; 10:e1001357. [PubMed: 22802725]

McKearin D, Spradling AC. Bag-of-marbles: a Drosophila gene required to initiate both male and female gametogenesis. Genes Dev. 1990; 4:2242–2251. [PubMed: 2279698]

McKearin D, Ohlstein B. A role for the Drosophila bag-of-marbles protein in the differentiation of cystoblasts from germline stem cells. Development. 1995; 121:2937–2947. [PubMed: 7555720]

Michel M, Raabe I, Kupinski AP, Perez-Palencia R, Bokel C. Local BMP receptor activation at adherens junctions in the Drosophila germline stem cell niche. Nat. Commun. 2011; 2:415. [PubMed: 21811244]

Narbonne-Reveau K, Besse F, Lamour-Isnard C, Busson D, Pret AM. fused regulates germline cyst mitosis and differentiation during Drosophila oogenesis. Mech. Dev. 2006; 123:197–209. [PubMed: 16516445]

Narimatsu M, Bose R, Pye M, Zhang L, Miller B, Ching P, Sakuma R, Luga V, Roncari L, Attisano L, Wrana JL. Regulation of planar cell polarity by Smurf ubiquitin ligases. Cell. 2009; 137:295–307. [PubMed: 19379695]

Ohlstein B, McKearin D. Ectopic expression of the Drosophila Bam protein eliminates oogenic germline stem cells. Development. 1997; 124:3651–3662. [PubMed: 9342057]

Orvedahl A, Sumpter R Jr, Xiao G, Ng A, Zou Z, Tang Y, Narimatsu M, Gilpin C, Sun Q, Roth M, Forst CV, Wrana JL, Zhang YE, Luby-Phelps K, Xavier RJ, Xie Y, Levine B. Image-based genome-wide siRNA screen identifies selective autophagy factors. Nature. 2011; 480:113–117. [PubMed: 22020285]

Podos SD, Hanson KK, Wang Y-C, Ferguson EL. The DSmurf ubiquitin-protein ligase restricts BMP signaling spatially and temporally during drosophila embryogenesis. Dev. cell. 2001; 1:567–578. [PubMed: 11703946]

Preat T, Therond P, Limbourg-Bouchon B, Pham A, Tricoire H, Busson D, Lamour-Isnard C. Segmental polarity in Drosophila melanogaster: genetic dissection of fused in a Suppressor of fused background reveals interaction with costal-2. Genetics. 1993; 135:1047–1062. [PubMed: 8307322]

Sangadala S, Boden SD, Viggeswarapu M, Liu Y, Titus L. LIM mineralization protein-1 potentiates bone morphogenetic protein responsiveness via a novel interaction with Smurf1 resulting in decreased ubiquitination of Smads. J. Biol. Chem. 2006; 281:17212–17219. [PubMed: 16611643]

Schulz C, Kiger AA, Tazuke SI, Yamashita YM, Pantalena-Filho LC, Jones DL, Wood CG, Fuller MT. A misexpression screen reveals effects of bag-ofmarbles and TGF beta class signaling on the Drosophila male germ-line stem cell lineage. Genetics. 2004; 167:707–723. [PubMed: 15238523]

Schwamborn JC, Khazaei MR, Puschel AW. The interaction of mPar3 with the ubiquitin ligase Smurf2 is required for the establishment of neuronal polarity. J. Biol. Chem. 2007a; 282:35259–35268. [PubMed: 17906294]

Schwamborn JC, Muller M, Becker AH, Puschel AW. Ubiquitination of the GTPase Rap1B by the ubiquitin ligase Smurf2 is required for the establishment of neuronal polarity. EMBO. J. 2007b; 26:1410–1422. [PubMed: 17318188]

Sekelsky JJ, Newfeld SJ, Raftery LA, Chartoff EH, Gelbart WM. Genetic characterization and cloning of mothers against dpp, a gene required for decapentaplegic function in drosophila melanogaster. Genetics. 1995; 139:1347–1358. [PubMed: 7768443]

Sheng XR, Posenau T, Gumulak-Smith JJ, Matunis E, Van Doren M, Wawersik M. Jak-STAT regulation of male germline stem cell establishment during Drosophila embryogenesis. Dev. Biol. 2009; 334:335–344. [PubMed: 19643104]

Shivdasani AA, Ingham PW. Regulation of stem cell maintenance and transit amplifying cell proliferation by TGF-β signaling in Drosophila spermatogenesis. Curr. Biol.: CB. 2003; 13:2065–2072.

Tsuneizumi K, Nakayama T, Kamoshida Y, Kornberg TB, Christian JL, Tabata T. Daughters against dpp modulates dpp organizing activity in Drosophila wing development. Nature. 1997; 389:627–631. [PubMed: 9335506]

Van Doren M, Williamson AL, Lehmann R. Regulation of zygotic gene expression in Drosophila primordial germ cells. Curr. Biol.: CB. 1998; 8:243–246.

Wang HR, Zhang Y, Ozdamar B, Ogunjimi AA, Alexandrova E, Thomsen GH, Wrana JL. Regulation of cell polarity and protrusion formation by targeting RhoA for degradation. Science. 2003; 302:1775–1779. [PubMed: 14657501]

Wang X, Harris RE, Bayston LJ, Ashe HL. Type IV collagens regulate BMP signalling in Drosophila. Nature. 2008; 455:72–77. [PubMed: 18701888]

Wiersdorff V, Lecuit T, Cohen SM, Mlodzik M. Mad acts downstream of Dpp receptors, revealing a differential requirement for dpp signaling in initiation and propagation of morphogenesis in the Drosophila eye. Development. 1996; 122:2153–2162. [PubMed: 8681796]

Wiesner S, Ogunjimi AA, Wang HR, Rotin D, Sicheri F, Wrana JL, Forman-Kay JD. Autoinhibition of the HECT-type ubiquitin ligase Smurf2 through its C2 domain. Cell. 2007; 130:651–662. [PubMed: 17719543]

Xia L, Jia S, Huang S, Wang H, Zhu Y, Mu Y, Kan L, Zheng W, Wu D, Li X, Sun Q, Meng A, Chen D. The fused/Smurf complex controls the fate of Drosophila germline stem cells by generating a gradient BMP response. Cell. 2010; 143:978–990. [PubMed: 21145463]

Yamashita M, Ying SX, Zhang GM, Li C, Cheng SY, Deng CX, Zhang YE. Ubiquitin ligase Smurf1 controls osteoblast activity and bone homeostasis by targeting MEKK2 for degradation. Cell. 2005; 121:101–113. [PubMed: 15820682]

Yamashita YM, Yuan H, Cheng J, Hunt AJ. Polarity in stem cell division: asymmetric stem cell division in tissue homeostasis. Cold Spring Harbor Perspect. Biol. 2010; 2:a001313.

Zhang J, Li L. BMP signaling and stem cell regulation. Dev. Biol. 2005; 284:1–11. [PubMed: 15963490]

Zhang Y, Chang C, Gehling DJ, Hemmati-Brivanlou A, Derynck R. Regulation of Smad degradation and activity by Smurf2, an E3 ubiquitin ligase. Proc. Natl. Acad. Sci. USA. 2001; 98:974–979. [PubMed: 11158580]

Zhu CH, Xie T. Clonal expansion of ovarian germline stem cells during niche formation in Drosophila. Development. 2003; 130:2579–2588. [PubMed: 12736203]

Zhu H, Kavsak P, Abdollah S, Wrana JL, Thomsen GH. A SMAD ubiquitin ligase targets the BMP pathway and affects embryonic pattern formation. Nature. 1999; 400:687–693. [PubMed: 10458166]

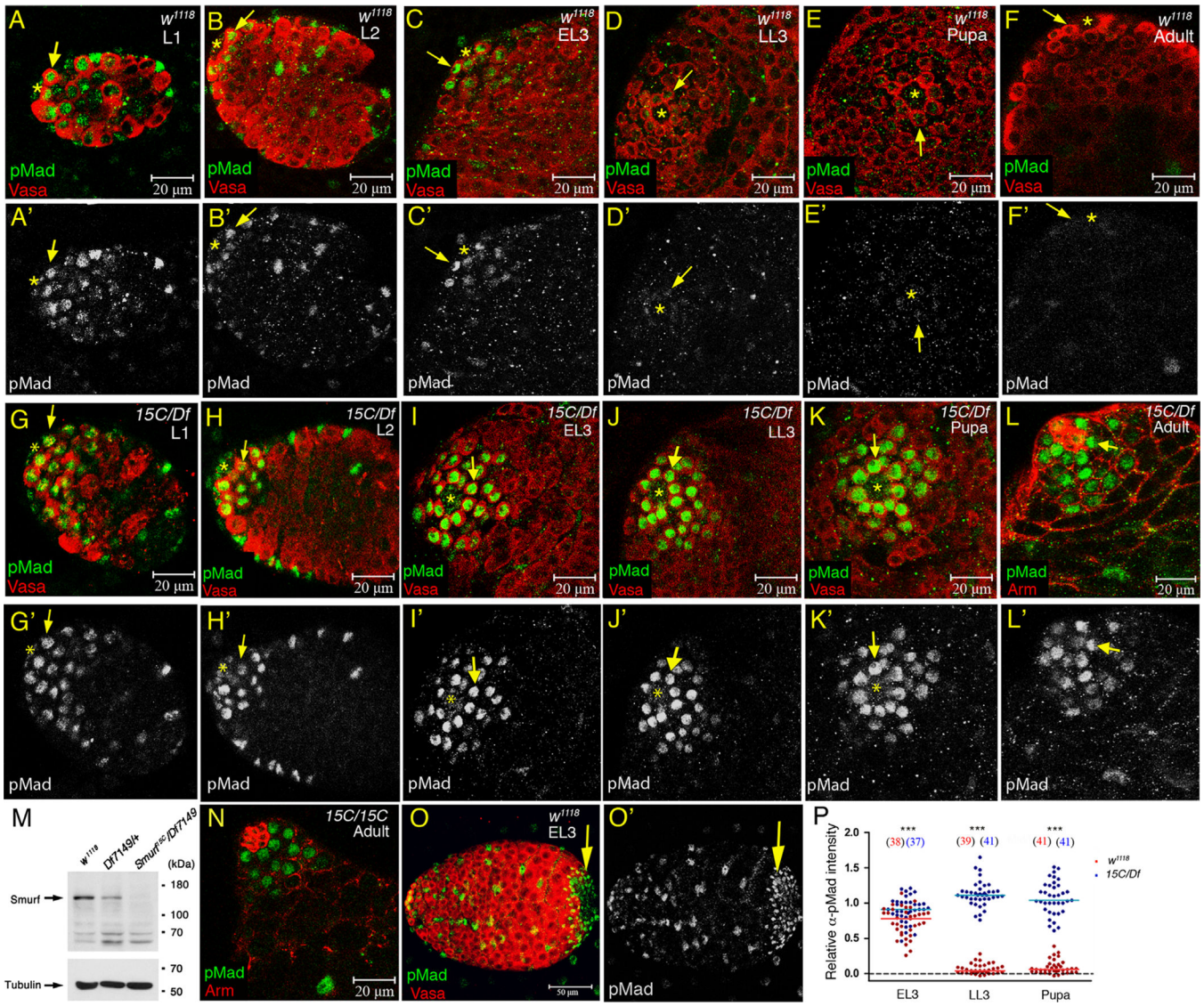

Figure 1.

Smurf is required for downregulation of pMad in GSCs and early germ cells during larval and pupal testis development. (A–K′) Testes immunostained for pMad (green), co-stained for Vasa (red) to mark germ cells. (Arrow) GSC. (Asterisk) hub. (A–F′) w^{1118} testes from L1 to adult. L1 testes were identified by the presence of hub (marked by anti-Arm staining, data not shown) at the anterior end of the gonads. (G–K′) $Smurf^{15C}/Df7149$ testes from L1 to early pupae. (L and L′) $Smurf^{15C}/Df7149$ 0–1 day adult testis immunostained for pMad (green), co-stained for Arm (red). (M) Western blot of adult testis extract with anti-DSmurf antibody (upper blot) and anti-Tubulin antibody (lower blot). Arrows in the upper and lower blots indicates the Smurf protein and tubulin protein bands, respectively. (N) $Smurf^{15C}/Smurf^{15C}$ 0–1 day adult testis immunostained for pMad (green), co-stained for Arm (red). (O and O′) w^{1118} EL3 testis immunostained for pMad (green), co-stained for Vasa (red). Arrows indicate the α-pMad-positive posterior terminal epithelial cells, which are used as an internal control for α-pMad immunofluoresence quantification. (P) Column scatter graph of the relative α-pMad intensity in GSCs in EL3, LL3 and 0–4 h APF testes. Horizontal lines represent the median value. Significance was evaluated by Mann–Whitney test. ***p<0.001. Numbers in the parenthesis are the numbers of GSC scored. The numbers of testes scored are ≥5 for each group at each time point.

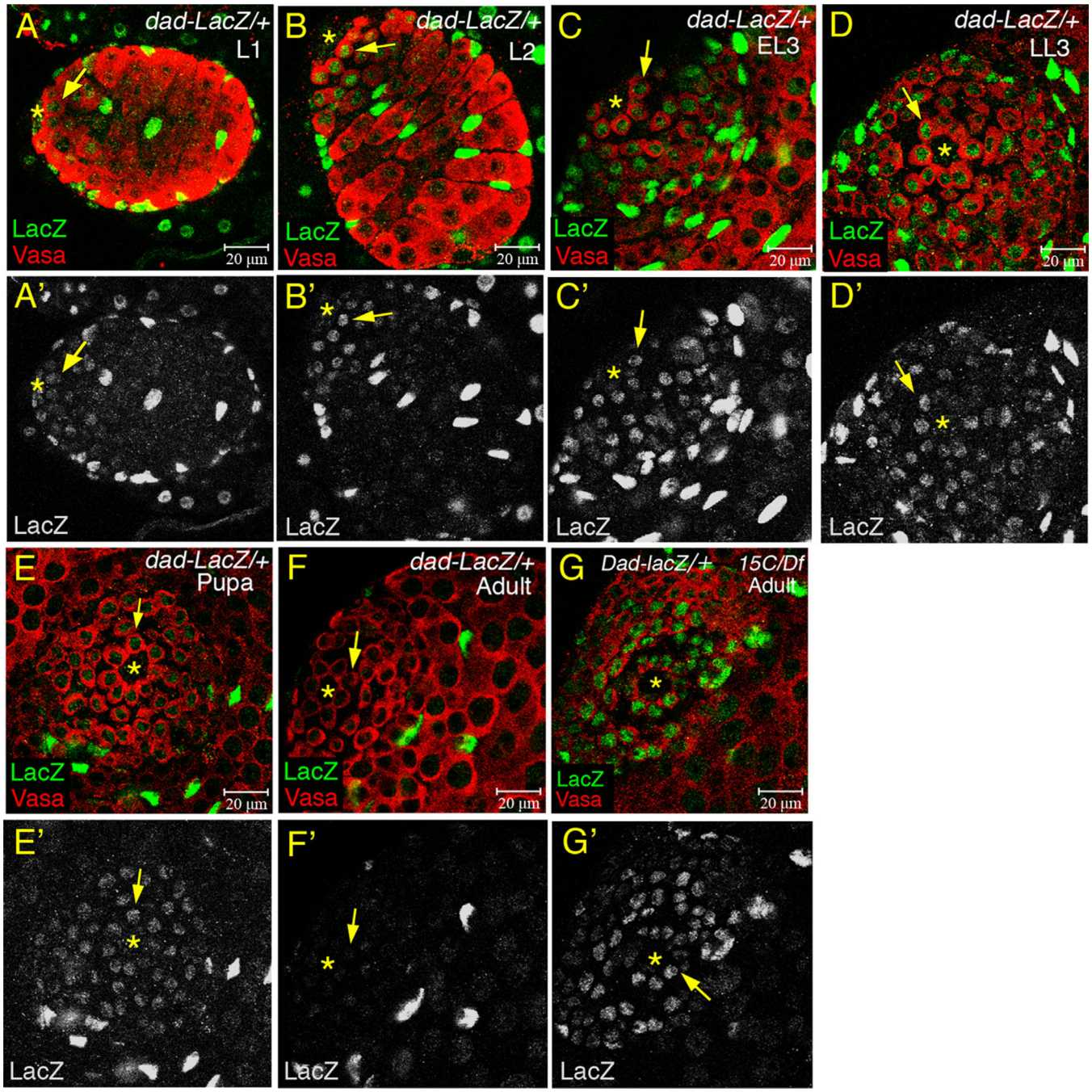

Figure 2.

Temporal downregulation of *Dad-LacZ* in early germ cells during testis maturation from pupae to adult. (A–G′) Testes immunostained for β-galactosidase (green), co-stained for Vasa (red). (Arrow) GSC. (Asterisk) hub. (A–E′) *Dad-LacZ* constantly expressed in GSCs and early germ cells from L1 to early pupae. (F and F′) *Dad-LacZ* expressed weakly in GSCs and early germ cells in 0–1 day adult testes. (G and G′) High levels of *Dad-LacZ* expression in GSCs and early germ cells in 0–1 day *Smurf*^{15C}/*Df7149* testes.

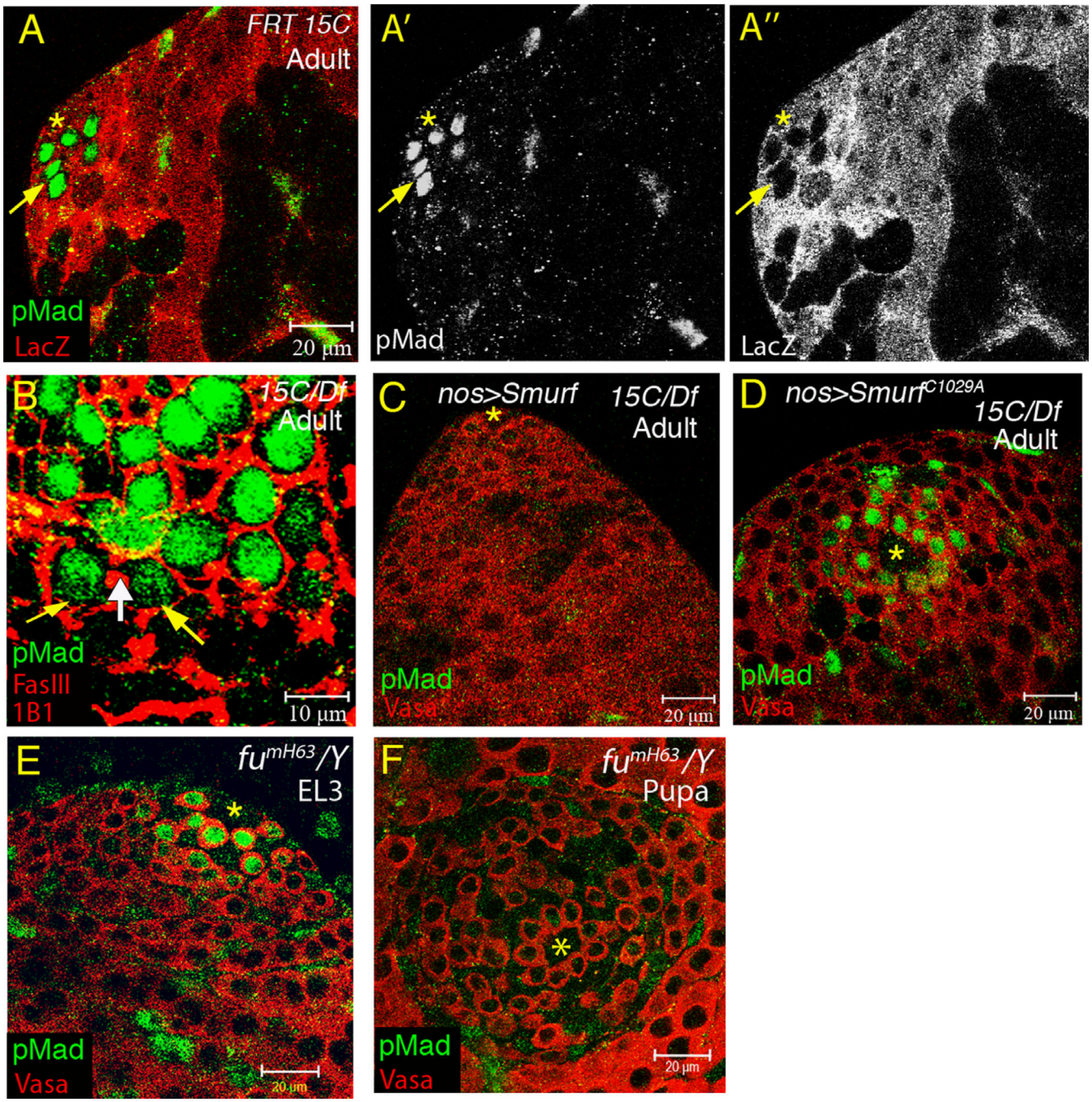

Figure 3.

Smurf is required autonomously in early germ cells for pMad downregulation. (A–A″) Testis immunostained with anti-pMad (green), co-stained with anti-LacZ (red) to mark *Smurf*^{15C} clones. Germ-cell autonomous accumulation of pMad in *Smurf*^{15C} clones in GSC, goniablast, and two-cell cyst (indicated by arrow). (B) 0–1 day *Smurf*^{15C}/*Df7149* testis immunostained for pMad (green), co-stained with anti-FasIII (red) to mark hub and mAb 1B1 (red) to mark spectrosome/fusome. The yellow arrows indicate the pMad-positive two-cell stage TA cells, that were identified by the presence of fusome (white arrow). (C and D) 0–1 day adult *Smurf*^{15C}/*Df7149* testes immunostained with anti-pMad (green), co-stained with anti-Vasa (red). pMad accumulation in early germ cells blocked by germ cell-specific expression of wild-type Smurf (C), but not E3 ligasedead SmurfC1029A (D).

(E and F) fu^{mH63}/Y testes immunostained with anti-pMad (green), co-stained with anti-Vasa (red). pMad levels in GSCs downregulated from EL3 (E) to pupae (F) in *fu* null mutant testes.

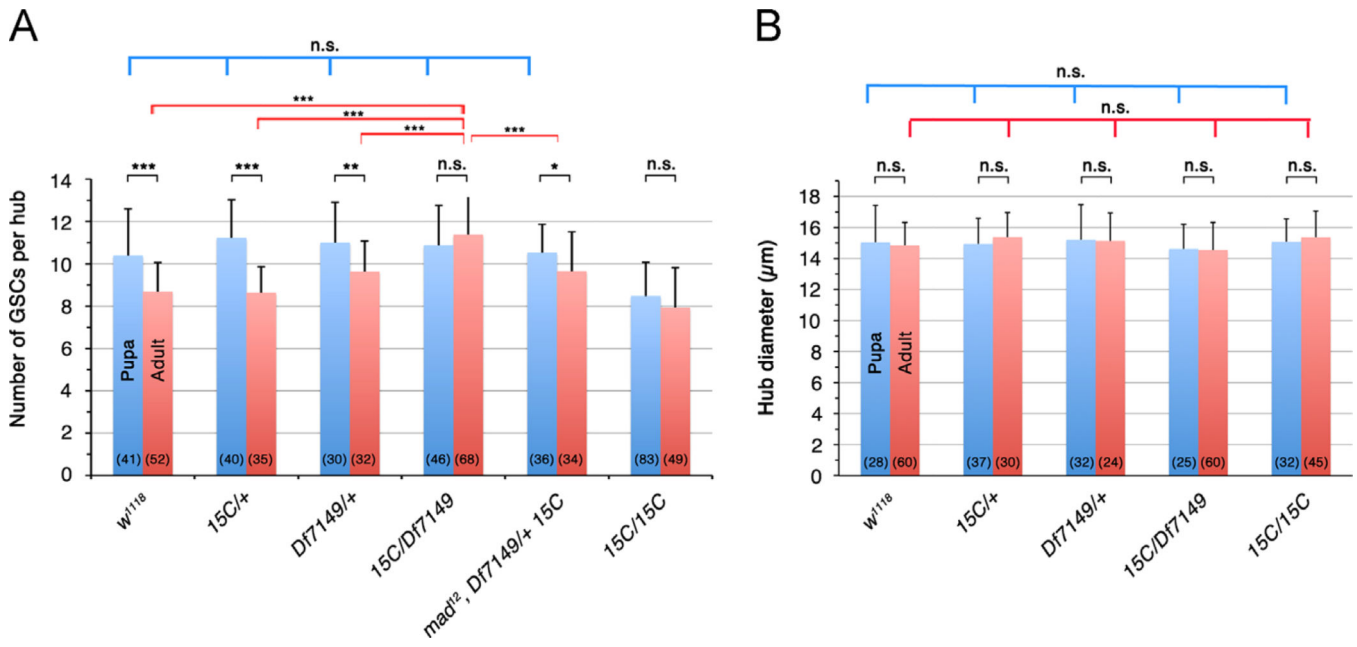

Figure 4.

Smurf controls the number of GSCs in adult testes. (A) GSC number in pupal (blue bar) and adult (red bar) testes. GSC numbers decreased from pupae to adult in wildtype (w^{1118}), *Smurf* heterozygous ($Smurf^{15C}$/+, *Df7149*/+) and mad^{12} *Df7149*/$Smurf^{15C}$ flies, but not in $Smurf^{15C}$/*Df7149* and $Smurf^{15C}$/$Smurf^{15C}$ mutants. Average (mean ± SD) was shown. Significance was calculated using two-tailed Student's *t*-test. ***p<0.001, **p<0.01, np<0.05. n.s.=not significant (p>0.05). Numbers in parenthesis represent the number of testes scored. (B) Hub diameter in pupal (0–4 h APF) and adult (0- to 1-day) testes, showing no significant change (p>0.05) between pupal and adult testes, or among w^{1118}, *Smurf* heterozygous and *Smurf* mutant gonads. Hub was identified as FasIII-positive cell cluster at testis apex.

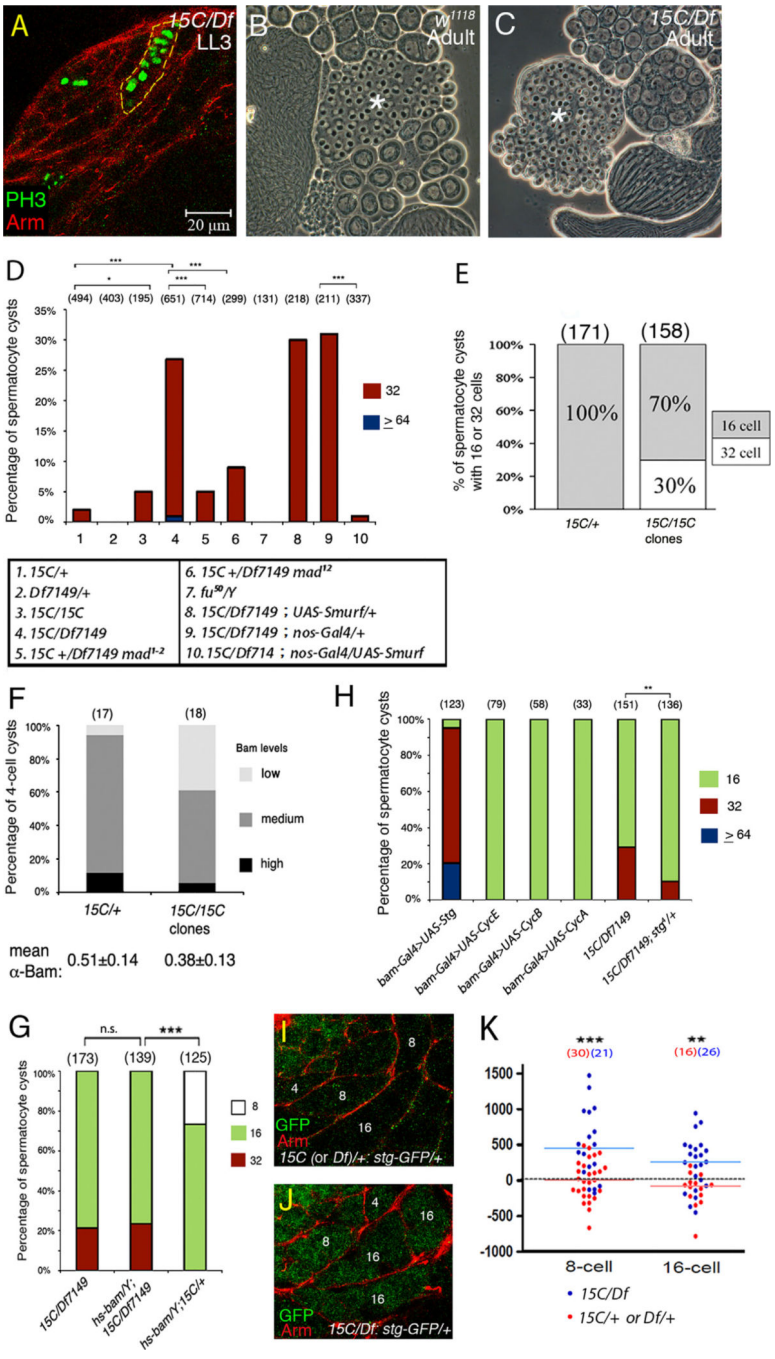

Figure 5.

Increased TA division numbers in *Smurf* mutant testes. (A) *Smurf*^{15C}/*Df7149* LL3 testes immunostained for mitotic marker PH3, costained with anti-Arm to label cyst cells. The dashed line outlines a cyst with >8 PH3-positive prophase-metaphase spermatogonia identified by Z-stacks of confocal images. (B) 64 Onion stage early round spermatids (asterisk) in a single cyst in *w*^{1118} adult testis. (C) Single cyst with 128 early spermatids (asterisk) in *Smurf*^{15C}/*Df7149* testis. (D) Percentage of cysts with 32 or ≥64 spermatocytes in adult testes. No 8-cell cysts were found in these samples. The percentage of 16-cell cysts is to minus the percentage of 32- and ≥64-cell cysts from the total (100%). Significance was evaluated by chi-square. ***p<0.001, np<0.05. (E) Germline clonal analysis of *Smurf*^{15C} in adult testes. 30% of the *Smurf*^{15C} spermatocyte cysts had 32 cells. Numbers in

parenthesis represent the numbers of spermatocyte cysts scored. (F) Percentage of 4-cell cysts with different levels of α-Bam intensity. Low-, medium- and high-Bam defined as the α-Bam intensity between 0% and 33%, 33% and 66%, and 66% and 100%, respectively, of the maximal α-Bam intensity in 4-cell cysts of +/+ control testes. The mean α-Bam intensity for *Smurf*^{15C}/+ and *Smurf*^{15C}/*Smurf*^{15C} 4-cell cysts is shown at the bottom. (G) Percentage of 8-, 16-, and 32-cell spermatocyte cysts in *Smurf* mutant adult testes expressing Bam under control of heat shock promoter. Significance was evaluated by chi-square. ***p<0.001. n.s.=not significant (p>0.05). (H) Percentage of 16-, 32- and 64-cell spermatocyte cysts in adult testes overexpressing cell cycle regulators, and in *Smurf*^{15C}/*Df7149* adult testes carrying one copy of *stg* null allele. Significance was evaluated by chi-square. **p<0.01. (I and J) LL3 *stg-GFP*^{YD0685} testes immunostained for GFP (green), co-stained for Arm (red) to label cysts. The 4-, 8-, and 16-cell cysts are marked with the numbers 4, 8, and 16, respectively. (K) Column scatter graph showing the α-GFP staining intensities of Stg-GFP in 8- and 16-cell cysts in *Smurf*^{15C}/*Df7149* or the sibling control *Smurf*^{15C}/+ or *Df7149*/+ LL3 testes. Horizontal lines represent the median value. Significance was evaluated by Mann–Whitney test. ***p<0.001, **p<0.01.

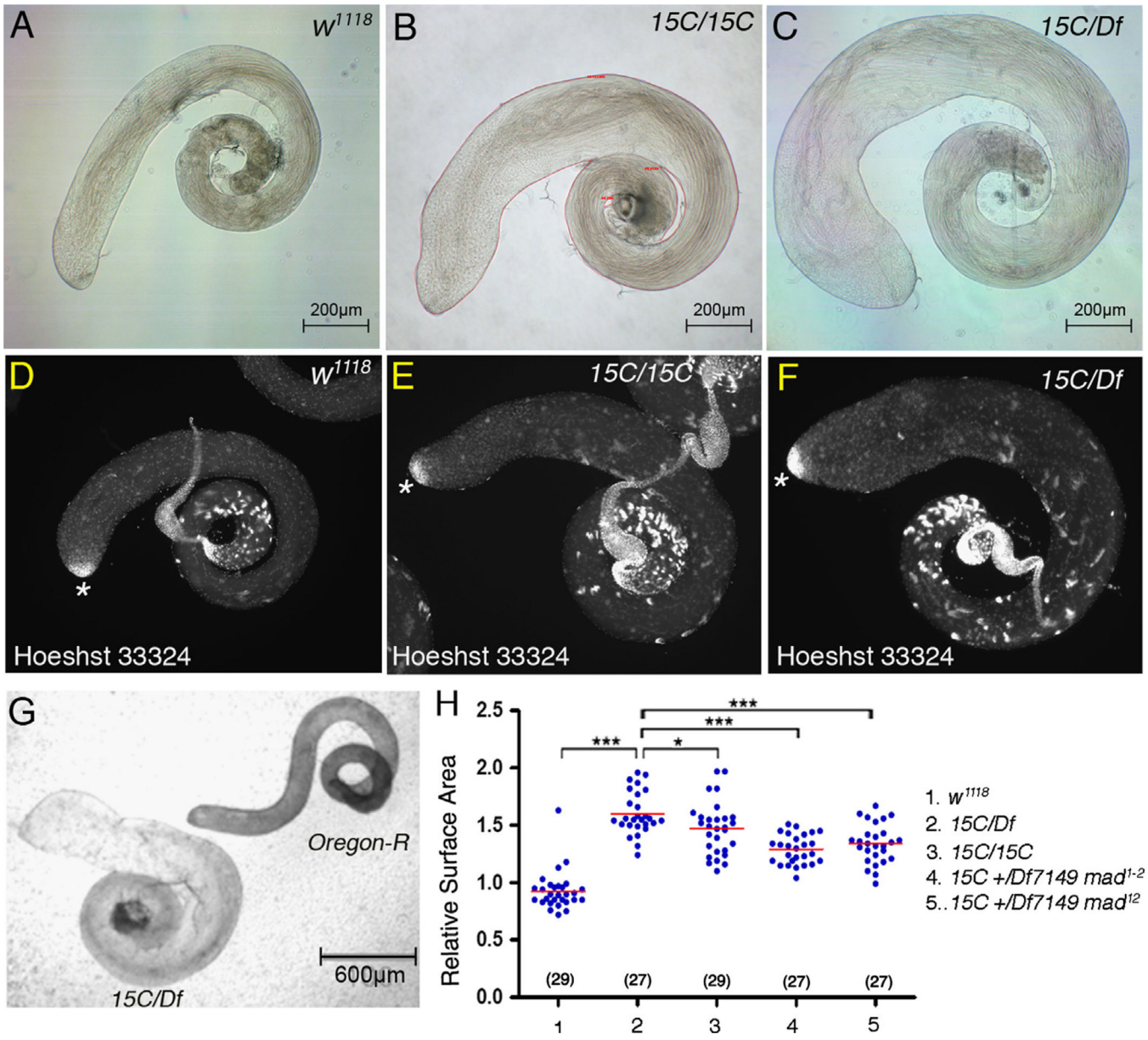

Figure 6.

Increased organ size in *Smurf* mutant testes. (A–C) Brightfield images of 0–1 day adult testes. Note increase in surface area in $Smurf^{15C}/Smurf^{15C}$ (B) and $Smurf^{15C}/Df7149$ (C) testes. The surface area of the adult testes is the area enclosed by the red line as shown in (B). (D–F) Adult testes stained with DNA dye Hoechst 33324. (D) Wildtype or (E and F) *Smurf* mutant testes, showing normal location of DNA-bright small germ cells at the testis tip (asterisks) and sperm with compacted and elongated nuclei. (G) Bright-field image of *Oregon-R* (right) and $Smurf^{15C}/Df7149$ (left) testes mounted on the same slide. (H) Column scatter graph showing the relative surface area normalized to *Oregon-R*. Horizontal lines represent the mean value. Significance was evaluated by two-tailed Students' *t*-test. ***$p<0.001$, *$p<0.05$.

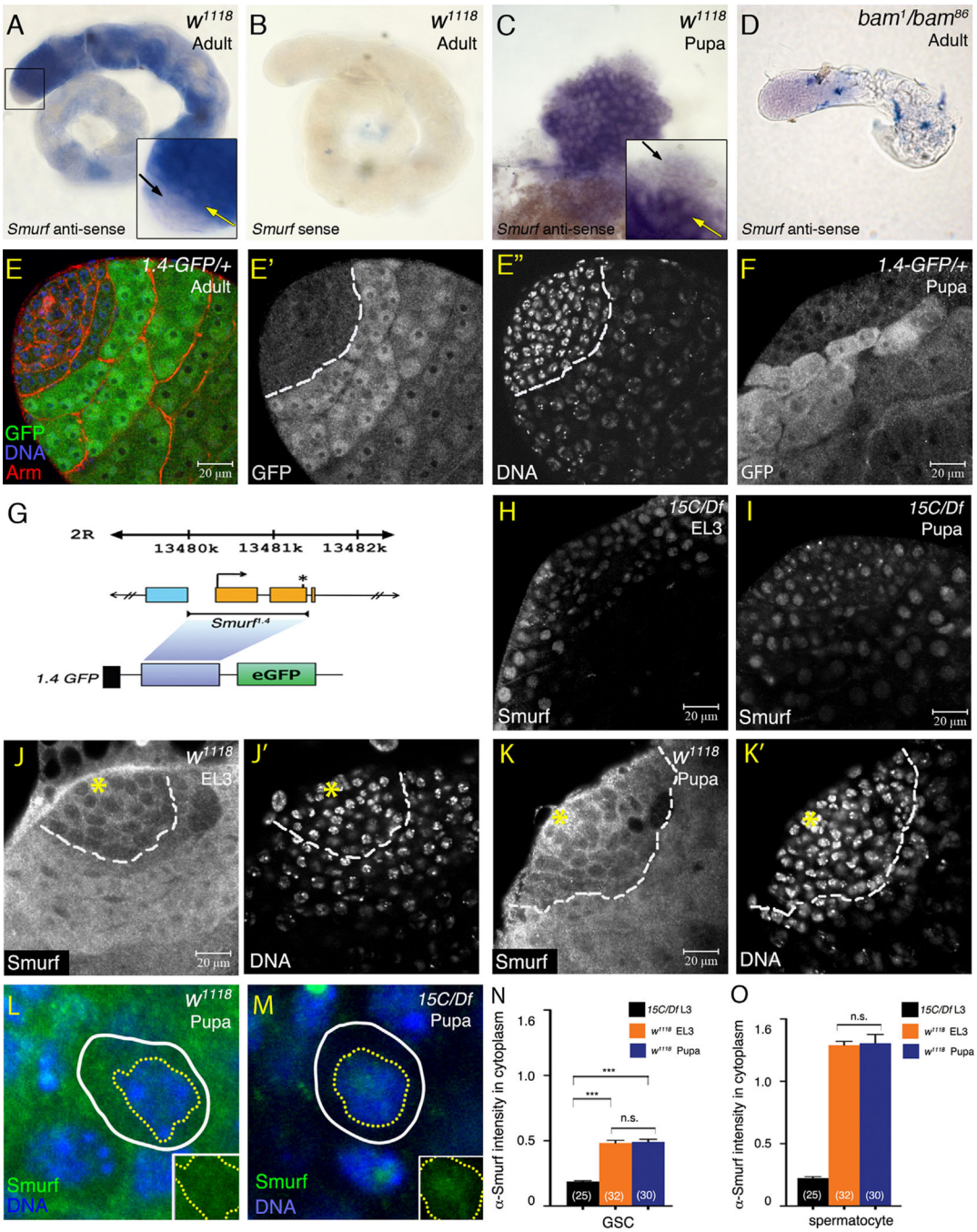

Figure 7.

Smurf mRNA and protein expressed in low levels in GSCs and spermatogonia. (A–B) Whole-mount in situ hybridization of 0–1 day adult testis with *Smurf* anti-sense (A) or sense (B) probes. (A) Weak *Smurf* mRNA expression detected in apical small cells (black arrow in inset), and robust *Smurf* mRNA expression initiated in enlarging spermatocytes (yellow arrow in inset). (B) *Smurf* sense probes: no signal. (C) Whole-mount in situ hybridization of early pupal testis with *Smurf* anti-sense probe. High and low levels of *Smurf* mRNA detected, respectively, in spermatocytes (yellow arrow) and apical small germ cells (black arrow). (D) Whole-mount in situ hybridization of 0–1 day *bam1*/*bam*^{86} adult testes with *Smurf* anti-sense probe. Strong *Smurf* mRNA expression eliminated with lack of spermatocytes in *bam* mutant testes. (E–E″) Testis immunostained for GFP (green), co-

stained for Arm (red) and Hoechst 33324 (blue). Expression of *Smurf* reporter*1.4-GFP* at high and low levels, respectively, in spermatocytes and spermatogonia in 0–1 day adult testis. White dashed lines in (E′ and E″) mark the boundary between GFP-low and GFP-high cells. (F) 0–4 h APF testis from *1.4-GFP*/+ pupae immunostained with anti-GFP antibody. (G) Schematic diagram of *Smurf* 1.4 kb genomic fragment and *1.4-GFP* reporter gene. The orange boxes represent *Smurf* exons. Light-blue box represents the exon of the nearest neighboring gene *CG30105*. Transcriptional and translational starts of *Smurf* are indicated by an arrow and an asterisk, respectively. (H and I) EL3 and early pupal $Smurf^{15C}/Df7149$ testes immunostained with anti-DSmurf antibody. Non-Smurf immunofluorecence observed in nucleus of all cells. (J–J′ and K–K′) w^{1118} EL3 and early pupal testes immunostained with anti-DSmurf antibody (white in J and K), and co-stained with Hoechst 33324 (white in J′ and K′). (Asterisk) hub. White dashed lines mark the boundary between Smurf-low and Smurf-high cells. (L and M) Enlarged figures of GSCs in wild-type (J) and $Smurf^{15C}/Df7149$ (K) testes immunostained with anti-DSmurf antibody. Yellow dotted and white solid lines outline the nucleus (DNA-positive) and the cell body (Vasa-positive), respectively. Insets show only the anti-DSmurf staining (green) in w^{1118} and $Smurf^{15C}/Df7149$ GSCs. The non-Smurf fluorescence in GSC nuclei appeared comparable between w^{1118} and $Smurf^{15C}/Df7149$. (N and O) Quantification of α-DSmurf immunofluorecent intensity in cytoplasm of GSCs (N) and spermatocytes (O). Significance was evaluated by two-tailed Student's *t*-test. ***$p<0.001$. n.s.=not significant ($p>0.05$).

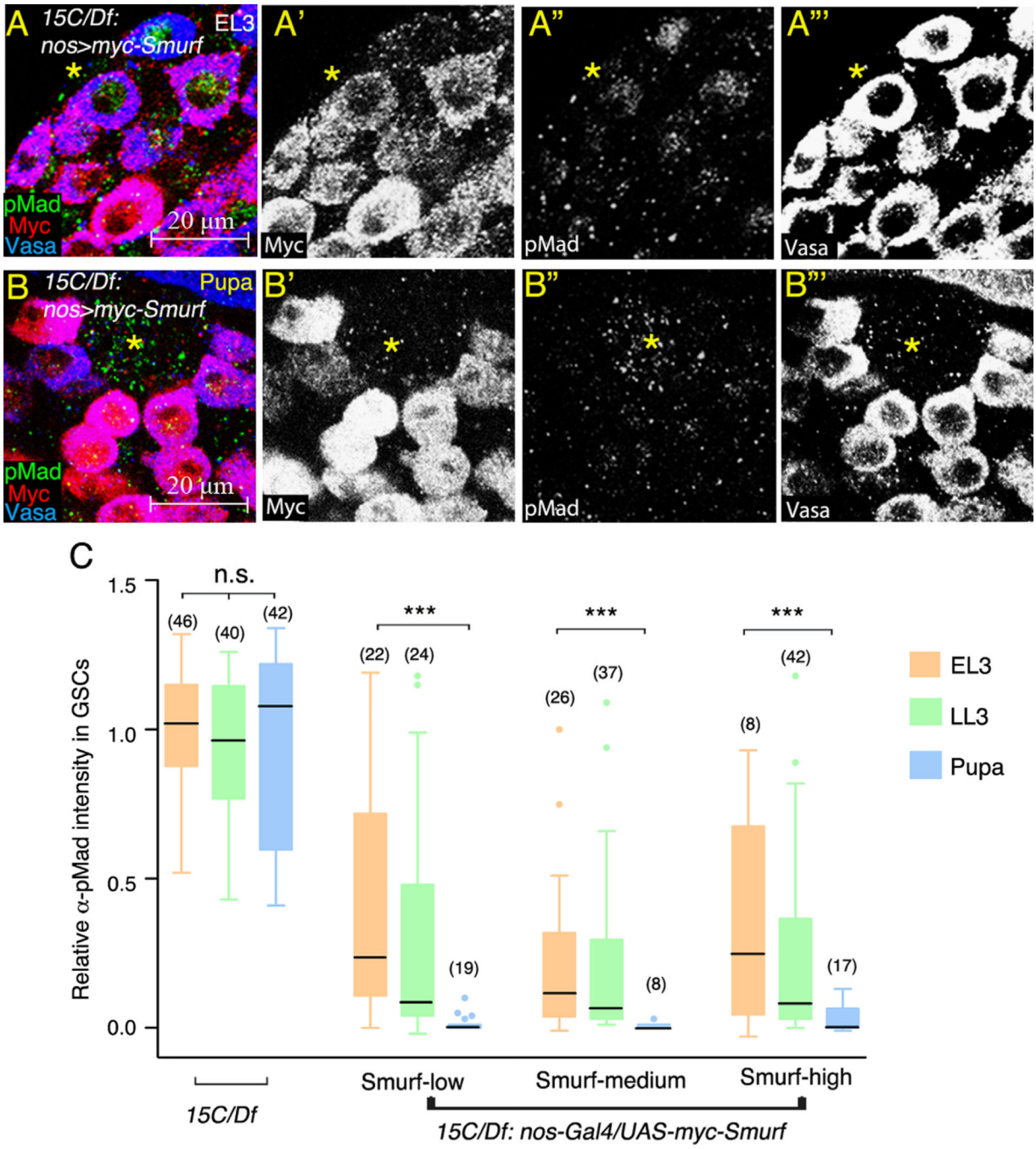

Figure 8.

Stage-dependent and concentration-independent suppression of pMad accumulation by exogenous Smurf. (A and B) Developing *Smurf*^{15C}*/Df7149*; *nos-Gal4/UAS-myc-Smurf* testes immunostained for pMad (green), co-stained with anti-Myc (red) and anti-Vasa (blue) antibodies. (Asterisk) hub. (A) EL3 testis. (B) 0–4 h APF testis. (C) Box-and-whisker plot of the relative α-pMad intensity in EL3, LL3 and pupal GSCs expressing low, medium or high levels of Myc-Smurf. Significantly higher levels of pMad observed in EL3 GSCs compared to pupal GSCs. The average α-pMad intensity in *Smurf*^{15C}*/Df7149* EL3 GSCs was set as 100%. Boxes present the first and third quartile and the horizontal lines within boxes represent the median value. The 1.5 × interquartile range and the outliers are shown by whisker and dots. Significance was evaluated by Mann–Whitney test.

***$p<0.001$. n.s.=not significant ($p>0.05$). Numbers in parenthesis represent the number of GSCs scored. At least eight testes were scored for each group at each time point.